11-3?-12
12012
1

JPL Publication 83-39, Rev. 3

Observation Model and Parameter Partials for the JPL VLBI Parameter Estimation Software "MASTERFIT"–1987

O. J. Sovers
J. L. Fanselow

(NASA-CR-182524) OBSERVATION MODEL AND PARAMETER PARTIALS FOR THE JPL VLBI PARAMETER ESTIMATION SOFTWARE MASTERFIT-1987 (Jet Propulsion Lab.) 66 p CSCL 03A

N88-16?2?

Unclas

G3/09 0126012

December 15, 1987

National Aeronautics and Space Administration

Jet Propulsion Laboratory
California Institute of Technology
Pasadena, California

TECHNICAL REPORT STANDARD TITLE PAGE

1. Report No. 83-39, Rev. 3	2. Government Accession No.	3. Recipient's Catalog No.
4. Title and Subtitle Observation Model and Parameter Partials for the JPL VLBI Parameter Estimation Software "MASTERFIT" -- 1987		5. Report Date December 15, 1987 6. Performing Organization Code
7. Author(s) O.J. Sovers and J.L. Fanselow		8. Performing Organization Report No.
9. Performing Organization Name and Address JET PROPULSION LABORATORY California Institute of Technology 4800 Oak Grove Drive Pasadena, California 91109		10. Work Unit No. 11. Contract or Grant No. NAS7-918 13. Type of Report and Period Covered JPL Publication
12. Sponsoring Agency Name and Address NATIONAL AERONAUTICS AND SPACE ADMINISTRATION Washington, D.C. 20546		14. Sponsoring Agency Code RE211 BC-314-30-41-81-35

15. Supplementary Notes

16. Abstract

This report is a revision of the document of the same title (1986), dated August 1, 1986, which it supersedes. Model changes during 1986 and 1987 included corrections for antenna feed rotation, refraction in modeling antenna axis offsets, and an option to employ improved values of the semiannual and annual nutation amplitudes. Partial derivatives of the observables with respect to an additional parameter (surface temperature) are now available. New versions of two figures representing the geometric delay are incorporated. The expressions for the partial derivatives with respect to the nutation parameters have been corrected to include contributions from the dependence of UT1 on nutation. The authors hope to publish revisions of this document in the future, as modeling improvements warrant.

17. Key Words (Selected by Author(s))	18. Distribution Statement		
Astronomy	Unclassified; unlimited		
19. Security Classif. (of this report) Unclassified	20. Security Classif. (of this page) Unclassified	21. No. of Pages	22. Price

JPL Publication 83-23, Rev. 3

Observation Model and Parameter Partials for the JPL VLBI Parameter Estimation Software "MASTERFIT"–1987

O. J. Sovers
J. L. Fanselow

December 15, 1987

NASA
National Aeronautics and Space Administration

Jet Propulsion Laboratory
California Institute of Technology
Pasadena, California

The research described in this publication was carried out by the Jet Propulsion Laboratory, California Institute of Technology, under a contract with the National Aeronautics and Space Administration.

Reference herein to any specific commercial product, process, or service by trade name, trademark, manufacturer, or otherwise does not constitute or imply its endorsement by the United States Government or the Jet Propulsion Laboratory, California Institute of Technology.

FOREWORD

This report is a revision of the document "MASTERFIT – 1986, dated August 1, 1986, which it supersedes. The model changes during 1986 and 1987 were rather minor. They included small corrections for feed rotation and refraction in modeling antenna axis offsets (Section 2.11, both previously neglected). Section 2.7 now includes the contributions from the dependence on the $UT1$ transformation to the nutation partials. A temporary optional model to correct semiannual and annual nutation terms has been installed. Finally, it is now possible to estimate the surface temperature when using the CfA mapping function (Section 4.3). Figures 1 and 2 have been redrawn to be more realistic representations of the geometric delay. A number of misprints have also been corrected. The present document corresponds to MASTERFIT version 350, which has been in use since September, 1987.

ACKNOWLEDGMENTS

O.J.S. appreciates the help of Chris Jacobs and Gabor Lanyi concerning the various antenna effects which are becoming more important as higher measurement accuracy is approached.

J.L.F. thanks Brooks Thomas and Polly Groth for their extensive proofreading and criticism of the V1.0 document. James Williams and Phil Callahan also provided important help. Jim, in particular, was responsible for the early development of the models for VLBI observations and has been invaluable in clarifying the many subtle issues involved. Phil contributed significantly to the section on the plasma effects.

In connection with the 1984 revisions, O.J.S. thanks Jim Williams for help with implementation of the IAU 1984 conventions. The pole tide model, as well as the nutation model changes, resulted from discussions with Chuck Yoder. Essentially all of the new troposphere model, as well as the corrections concerning higher-order ionospheric effects, are due to Gabor Lanyi. Clarification of the effects of light transit time on gravitational bending was made by George Pataakos of the University of Idaho in the course of his stay at JPL during the summer of 1984.

Many colleagues in Section 335 contributed to improvements and clarifications of the MASTERFIT code over the years. Among them are Steve Allen, Marshall Eubanks, Chris Jacobs, Jean-François Lestrade, Kurt Liewer, Jean Patterson, Brooks Thomas, and Bob Treuhaft.

ABSTRACT

This report is a revision of the document of the same title (1986), dated August 1, 1986, which it supersedes. Model changes during 1986 and 1987 included corrections for antenna feed rotation, refraction in modeling antenna axis offsets, and an option to employ improved values of the semiannual and annual nutation amplitudes. Partial derivatives of the observables with respect to an additional parameter (surface temperature) are now available. New versions of two figures representing the geometric delay are incorporated. The expressions for the partial derivatives with respect to the nutation parameters have been corrected to include contributions from the dependence of $UT1$ on nutation. The authors hope to publish revisions of this document in the future, as modeling improvements warrant.

CONTENTS

1. INTRODUCTION 1

2. GEOMETRIC DELAY 2
   2.1 TIME INTERVAL FOR THE PASSAGE OF A WAVE FRONT BETWEEN TWO STATIONS 3
   2.2 TIME INFORMATION 10
   2.3 STATION LOCATION TIME DEPENDENCE 11
   2.4 TIDAL EFFECTS 12
      2.4.1 Solid Earth Tides 12
      2.4.2 Ocean Loading 13
      2.4.3 Atmosphere Loading 14
      2.4.4 Pole Tide 15
   2.5 TRANSFORMATION FROM TERRESTRIAL TO CELESTIAL COORDINATE SYSTEMS 16
   2.6 UT1 AND POLAR MOTION 16
   2.7 NUTATION 20
   2.8 PRECESSION 25
   2.9 PERTURBATION ROTATION 25
   2.10 EARTH ORBITAL MOTION 26
   2.11 ANTENNA GEOMETRY 29
   2.12 PARTIAL DERIVATIVES OF DELAY WITH RESPECT TO GEOMETRIC MODEL PARAMETERS 34

3. CLOCK MODEL 41

4. TROPOSPHERE MODEL 42
   4.1 CHAO MAPPING FUNCTION 43
   4.2 LANYI MAPPING FUNCTION 43
   4.3 CFA MAPPING FUNCTION 46

5. IONOSPHERE MODEL 47

6. MODELING THE PHASE DELAY RATE (FRINGE FREQUENCY) 52

7. PHYSICAL CONSTANTS USED 53

8. POSSIBLE IMPROVEMENTS TO THE CURRENT MODEL 54

9 REFERENCES 55

APPENDICES
   A. EQUIVALENCE OF TWO METHODS OF CORRECTING FOR GRAVITATIONAL BENDING 58
   B. MASTERFIT PARAMETERS 59

Figures

1. Geometry for calculating the transit time of a plane wave front 4
2. Geometry for calculating the transit time of a curved wave front 5
3. A schematic representation of the geodesic connecting two points in the presence of a gravitational mass 7
4. A schematic representation of the motion of a gravitating object during the transit time of a signal from the point of closest approach to reception by an antenna 8
5. A generalized schematic representation of the geometry of a steerable antenna 30
6. Schematic representations of the four major antenna geometries used in VLBI 32
7. The geometry of the spherical ionospheric shell used for ionospheric corrections 50

Tables

I. Plate Rotation Velocities: Minster-Jordan AM0-2 Model 11
II. Periodic Tidally Induced Variations in UT1 with Periods Less than 35 Days 19
III. 1980 IAU Theory of Nutation 22
IV. Dependence of the Constants a and b on Tropospheric Model Parameters 45
B.I. Glossary of MASTERFIT Parameters 59

SECTION 1

INTRODUCTION

In applications of radio interferometry to geodynamics and astrometry, observed values of delay and delay rate obtained from observations of many different radio sources must be passed simultaneously through a multiparameter estimation routine to extract the significant model parameters. As the accuracy of radio interferometry has improved, increasingly complete models for the delay and delay rate observables have been developed. This report describes the current status of the delay model used in the Jet Propulsion Laboratory multiparameter estimation program "MASTERFIT". It is assumed that the reader has at least a cursory knowledge of the principles of VLBI.

The delay model is the sum of four major model components: geometry, clock, troposphere, and ionosphere. Sections 2 through 5 present our current models for these components, as well as their partial derivatives with respect to parameters that are to be adjusted by multiparameter fits to the data. The longest section (2) deals with the geometric delay and covers the topics of time definitions, tidal effects, coordinate frames, Earth orientation (universal time and polar motion), nutation, precession, Earth orbital motion, wave front curvature, gravitational bending, and antenna offsets. Section 6 describes the technique used to obtain the delay rate model from the delay model. Section 7 gives the values of physical constants used in MASTERFIT, while section 8 outlines model improvements that may be required by more accurate data in the future.

SECTION 2

GEOMETRIC DELAY

The geometric delay is that interferometer delay which would be measured by perfect instrumentation, perfectly synchronized, if there were a perfect vacuum between the sources observed and the instrumentation. Typically this delay can be as great as 0.02 second for Earth-fixed baselines, and changes rapidly (up to 1.5 μsec per second) as the Earth rotates. In general this component of the delay is by far the largest component of the observed delay. The main complexity of this portion of the model arises from the numerous coordinate transformations necessary to relate the reference frame used for locating the radio sources to the Earth-fixed reference frame in which station locations are represented.

In the following we will assume, unless otherwise stated, that "celestial reference frame" means a reference frame in which there is no net proper motion of the extragalactic radio objects which are observed by the interferometer. This is only an approximation to some truly "inertial" frame. Currently, this celestial frame implies a geocentric, equatorial frame with the equator and equinox of J2000 as defined by the 1976 IAU conventions with the 1980 nutation series (Seidelmann, 1982, and Kaplan, 1981).

In this equatorial frame, some definition of the origin of right ascension must be made. We will not discuss that in this paper, since one definition is at most a rotation from some other definition, and can be applied at any time. The important point is that consistent definitions must be used throughout the model development. The need for this consistency will, in all probability, eventually lead to our defining the origin of right ascension by means of the JPL planetary ephemerides, followed by our using interferometric observations of both natural radio sources and spacecraft at planetary encounters as a means of connecting the planetary and the radio reference frames.

Also, unless otherwise stated, we will mean by "terrestrial reference frame" some reference frame tied to the mean surface features of the Earth. Currently, we are using a right-handed version of the CIO reference system with the pole defined by the 1903.0 pole. In practice, this is accomplished by defining the position of one of the interferometric observing stations (generally DSS 14 at the Goldstone Deep Space tracking complex) and then by measuring the positions of the other stations under a constraint. This constraint is that the determinations of Earth orientation agree on the average with the Bureau International de l'Heure (BIH) (1982) measurements of the Earth's orientation over some substantial time interval (≈ years). This procedure, or its functional equivalent, is necessary since the interferometer is sensitive only to the baseline vector as measured in the celestial frame. The VLBI technique is purely geometric and does not have any preferred origin point directly based on the structure of the Earth. The rotation of the Earth does, however, provide a preferred direction in space which can be associated indirectly with the surface features of the Earth.

In contrast, geodetic techniques which involve the use of satellites, or the Moon, are sensitive to the center of mass of the Earth as well as the spin axis. Thus, those techniques require only a definition of the origin of longitude. We anticipate that laser ranging to the retroreflectors on the Moon (LLR) will allow a realizable practical definition of a terrestrial frame, accurately positioned relative to a celestial frame tied to the planetary ephemerides. Co-location of the laser stations with the interferometer elements will be required to achieve this, however.

Careful definitions and experiments of this sort will be required to realize a coordinate system of centimeter accuracy. In the meantime, we must establish interim coordinate systems carefully enough so that we do not degrade the intrinsic accuracy of the interferometer data by introducing "model noise".

Several equivalent formulations are possible for the calculation of geometric delay. Our interest in also using this technique for radio sources within the Solar System has led to the formulation presented here. The problem of calculating the time delay for these "local" sources is simplified if the calculations are carried out in a frame at rest relative to the center of mass of the Solar System. For our present data, Lorentz transformations adequately account for the relativistic effects which arise from the relative motion of the objects involved. General relativity is required only for those effects which are associated with the bending of ray paths by the more massive objects in the Solar System.

For the above reasons we have performed the calculation as outlined below:

1. Specify the coordinates of the two stations as measured in an Earth-fixed frame at the time that the wave front intersects station #1. Let this time be t_1' as measured by a clock in the Earth-fixed frame.
2. Modify the station locations for Earth-fixed effects such as solid Earth tides, tectonic motion, and other local station motion.
3. Transform these station locations to a celestial coordinate system with the origin at the center of the Earth, but moving with the Earth. This is a composite of 10 separate rotations, represented by a rotation matrix $Q(t)$.
4. Perform a Lorentz transformation of these station locations from the Earth-fixed frame to a frame at rest relative to the center of mass of the Solar System, and rotationally aligned with the celestial geocentric frame.
5. In this Solar System barycentric frame, compute the time interval for the passage of the specified wave front from station #1 to station #2. Include the effects of the curvature of the wave front due to the finite distance of the source if relevant. Also, add in the effects of the differential gravitational retardation of the signal received by way of the two separate interferometer ray paths.
6. Perform a Lorentz transformation of this calculated geometric delay back to the celestial geocentric frame moving with the Earth. Except for negligible effects discussed later, this produces the model for the geometric portion of the observed delay.
7. To this geometric delay, add the contributions due to clock offsets, to tropospheric delays, and to the effects of the ionosphere on the signal (see sections 3 through 5 below).

The remainder of this section provides the details for the first six steps of the general outline above. Note that we have invoked only special relativistic coordinate transformations. Gravitational effects are incorporated as correction terms added on to the geometric delay once it is calculated in the Solar System barycenter.

2.1 TIME INTERVAL FOR THE PASSAGE OF A WAVE FRONT BETWEEN TWO STATIONS

The fundamental part of the geometric model is the calculation (step #5 above) of the time interval for the passage of a wave front from station #1 to station #2. We actually do that calculation in a coordinate frame at rest relative to the center of mass of the Solar System. However, the basic formulation is independent of the frame used. This part of the model is presented first to provide a context for the subsequent sections, all of which are heavily involved with the details of time definitions and coordinate transformations. We will use the same subscript and superscript notation which is used in section 2.10 below to refer to the station locations as seen by an observer at rest relative to the center of mass of the Solar System.

First, we calculate the interval that would be observed if the wave front were planar. Next, we generalise this calculation to a curved wave front, and finally, we take into account the incremental effect which results from the fact that we must consider wave fronts that propagate through the various gravitational potential wells in the Solar System. To start, consider the case of a plane wave moving in the direction, $\hat{\mathbf{k}}$, with station 2 having a mean velocity, $\boldsymbol{\beta}_2$, as shown in figure 1. The time delay is the time it takes the wave front to move the distance l. Measured in units of time, this distance is the sum of the two solid lines perpendicular to the wave front in figure 1:

$$t_2^* - t_1 = \hat{\mathbf{k}} \cdot [\mathbf{r}_2(t_1) - \mathbf{r}_1(t_1)] + \hat{\mathbf{k}} \cdot \boldsymbol{\beta}_2 |t_2^* - t_1| \tag{2.1}$$

This leads to the following expression for the geometric delay:

$$t_2^* - t_1 = \frac{\hat{\mathbf{k}} \cdot [\mathbf{r}_2(t_1) - \mathbf{r}_1(t_1)]}{1 - \hat{\mathbf{k}} \cdot \boldsymbol{\beta}_2} \tag{2.2}$$

In the case of a signal generated by a radio source within the Solar System it is necessary to include the effect of the curvature of the wave front. As depicted in figure 2, let a source irradiate two Earth-fixed stations whose positions are given by $\mathbf{r}_i(t)$ relative to the Earth's center. The position of the Earth's center, $\mathbf{R}_c(t_1)$, as a function of signal reception time, t_1, at station #1 is measured relative to the position of the emitter at the time, t_e, of emission of the signal received at time t_1. While this calculation is actually done in the Solar System barycentric coordinate system, the development that follows is by no means restricted in applicability to that frame.

Suppose that a wave front which leaves the source at time t_e reaches station #1 at time t_1 and arrives at station #2 at time t_2^*. The geometric delay in this frame will be given by:

$$\tau = t_2^* - t_1 = |\mathbf{R}_2(t_2^*)| - |\mathbf{R}_1(t_1)| \tag{2.3}$$

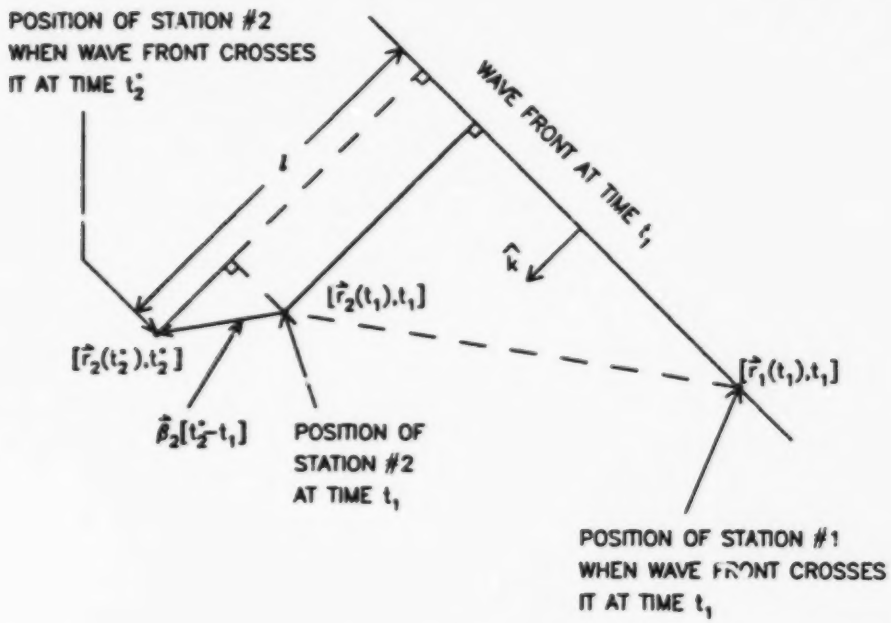

Figure 1. Geometry for calculating the transit time of a plane wave front

where all distances are again measured in units of light travel time. If we approximate the velocity of station #2 by

$$\boldsymbol{\beta}_2 = \frac{\mathbf{R}_2(t_2^*) - \mathbf{R}_2(t_1)}{t_2^* - t_1} \tag{2.4}$$

and use the relation

$$\mathbf{R}_i(t_1) = \mathbf{R}_c(t_1) + \mathbf{r}_i(t_1) \tag{2.5}$$

we obtain:

$$\begin{aligned} \tau &= |\mathbf{R}_c(t_1) + \mathbf{r}_2(t_1) + \boldsymbol{\beta}_2\tau| - |\mathbf{R}_c(t_1) + \mathbf{r}_1(t_1)| \\ &= R_c(t_1)\ \left[\ |\hat{\mathbf{R}}_c + \boldsymbol{\epsilon}_2| - |\hat{\mathbf{R}}_c + \boldsymbol{\epsilon}_1|\ \right] \end{aligned} \tag{2.6}$$

where

$$\boldsymbol{\varepsilon}_2 = \frac{\mathbf{r}_2(t_1) + \boldsymbol{\beta}_2 \tau}{R_c(t_1)} \tag{2.7}$$

and

$$\boldsymbol{\varepsilon}_1 = \frac{\mathbf{r}_1(t_1)}{R_c(t_1)} \tag{2.8}$$

For ε_1 and $\varepsilon_2 \leq 10^{-4}$, we need to keep only terms of order ε^3 in a sixteen-place machine in order to expand the expression for τ in equation (2.6). This gives us:

$$\tau = \frac{\hat{\mathbf{R}}_c \cdot [\mathbf{r}_2(t_1) - \mathbf{r}_1(t_1)]}{[1 - \hat{\mathbf{R}}_c \cdot \boldsymbol{\beta}_2]} + \frac{R_c \Delta_c(\tau)}{2\,[1 - \hat{\mathbf{R}}_c \cdot \boldsymbol{\beta}_2]} \tag{2.9}$$

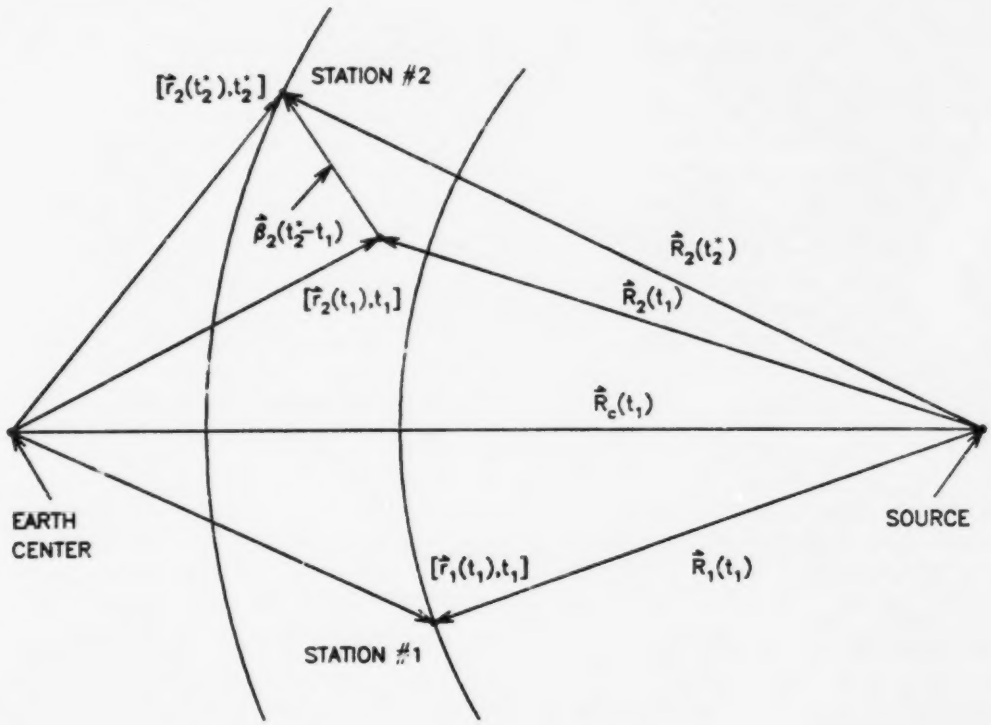

Figure 2. Geometry for calculating the transit time of a curved wave front

where to order ε^3

$$\Delta_c(\tau) = [\varepsilon_2^2 - \varepsilon_1^2] - [(\hat{\mathbf{R}}_c \cdot \boldsymbol{\varepsilon}_2)^2 + (\hat{\mathbf{R}}_c \cdot \boldsymbol{\varepsilon}_1)^2 + (\hat{\mathbf{R}}_c \cdot \boldsymbol{\varepsilon}_2)^3 - (\hat{\mathbf{R}}_c \cdot \boldsymbol{\varepsilon}_2)\varepsilon_2^2 - (\hat{\mathbf{R}}_c \cdot \boldsymbol{\varepsilon}_1)^3 + (\hat{\mathbf{R}}_c \cdot \boldsymbol{\varepsilon}_1)\varepsilon_1^2] \tag{2.10}$$

The first term in (2.9) is just the plane wave approximation, *i.e.*, as $R_c \rightarrow \infty$, $\hat{\mathbf{R}}_c \rightarrow \hat{\mathbf{k}}$, with the second term in brackets in (2.10) approaching zero as r^2/R_c. Given that the ratio of the first term to the second term is $\approx r/R_c$, wave front curvature is not calculable in a sixteen-place machine for $R > 10^{16} \times r$. For Earth-fixed baselines, the requirement that the effects of curvature be less than 0.01

cm implies that the above formulation (2.10) must be used for $R < 3.6 \times 10^{14}$ km, or approximately 2×10^6 astronomical units.

The procedure for the solution of (2.9) is iterative for $\varepsilon < 10^{-4}$, using the following:

$$\tau_n = \tau_0 + \frac{R_c \Delta_c(\tau_{n-1})}{2[1 - \hat{\mathbf{R}} \cdot \boldsymbol{\beta}_2]} \tag{2.11}$$

where

$$\tau_0 = \tau_{plane\ wave} \tag{2.12}$$

For $\varepsilon > 10^{-4}$, directly iterate on the equation (2.6) itself, using the procedure:

$$\tau_n = R_c|\hat{\mathbf{R}}_c + \boldsymbol{\varepsilon}_2(\tau_{n-1})| - R_c|\hat{\mathbf{R}}_c + \boldsymbol{\varepsilon}_1| \tag{2.13}$$

where again τ_0 is the plane wave approximation.

Because of the retardation of a light signal propagating in a gravitational potential well, the computed value for the differential time of arrival of the signals at $\mathbf{r}_1(t_1)$ and $\mathbf{r}_2(t_2^*)$ must be incremented from the value calculated above. For the geometry illustrated in figure 3, the required delay increment, Δ_{Gp}, is given by Moyer (1971):

$$\Delta_{Gp} = \frac{(1+\gamma_{PPN})\mu_p}{c^3} \left[\ln\left[\frac{r_s + r_2(t_2^*) + r_{s2}}{r_s + r_2(t_2^*) - r_{s2}}\right] - \ln\left[\frac{r_s + r_1(t_1) + r_{s1}}{r_s + r_1(t_1) - r_{s1}}\right] \right] \tag{2.14}$$

where r_{si} is defined as:

$$r_{si} = |\mathbf{r}_i(t_i) - \mathbf{r}_s(t_e)| \tag{2.15}$$

As will be shown below, some care must be taken in defining the positions given by $\mathbf{r}_s$, $\mathbf{r}_2(t_2^*)$, and $\mathbf{r}_1(t_1)$. We have chosen as the origin the position of the gravitational mass at the time of closest approach of the received signal to that object. The position, $\mathbf{r}_s$, of the source relative to this origin is the position of that source at the time, t_e, of the emission of the received signal. Likewise, the position, $\mathbf{r}_i(t_i)$, of the i^{th} receiver is its position in this coordinate system at the time of reception of the signal. Even with this care in the definition of the relative positions, we are making an approximation, and implicitly assuming that such an approximation is no worse than the approximations used by Moyer (1971) to obtain (2.14). Here γ_{PPN} is the γ factor in the parameterized post-Newtonian gravitational theory:

$$\gamma_{PPN} = \frac{1+\omega}{2+\omega} \tag{2.16}$$

where ω is the coupling constant of the scalar field. For general relativity, $\gamma_{PPN} = 1$, i.e., $\omega \to \infty$. However, we allow γ_{PPN} to be a "solve-for" constant so that by setting $\gamma_{PPN} = -1$, we also have the option of "turning off" the effects of general relativity on the estimate of the delay. This proves useful for software development. The gravitational constant, μ_p, is

$$\mu_p = Gm_p \tag{2.17}$$

where G is the universal gravitational constant, and m_p is the mass of the body. Dropping the time arguments, we have:

$$\Delta_{Gp} = \frac{(1+\gamma_{PPN})\mu_p}{c^3} \ln\left[\left[\frac{r_s + r_2 + r_{s2}}{r_s + r_1 + r_{s1}}\right]\left[\frac{r_s + r_1 - r_{s1}}{r_s + r_2 - r_{s2}}\right]\right] \tag{2.18}$$

This formulation is fine for $r_s \approx r_1 \approx r_{s1}$, but can be put in a computationally better form for the case of distant sources with closely spaced VLBI receivers, i.e., $|\mathbf{r}_2 - \mathbf{r}_1|/r_1 \to 0, r_1/r_s \to 0$. For these sources, expand Δ_{Gp} in terms of r_1/r_s, r_{s1}/r_s, and make use of the relationship

$$r_{s1} = |\mathbf{r}_s^2 - 2\mathbf{r}_s \cdot \mathbf{r}_1 + \mathbf{r}_1^2|^{1/2} \approx r_s[1 - \mathbf{r}_1 \cdot \hat{\mathbf{r}}_s] \tag{2.19}$$

This leads to

$$\Delta_{Gp} = \frac{(1+\gamma_{PPN})\mu_p}{c^3} \cdot \ln\left[\frac{r_1 + \mathbf{r}_1 \cdot \hat{\mathbf{r}}_s}{r_2 + \mathbf{r}_2 \cdot \hat{\mathbf{r}}_s}\right] \tag{2.20}$$

for $r_1/r_s \to 0$.

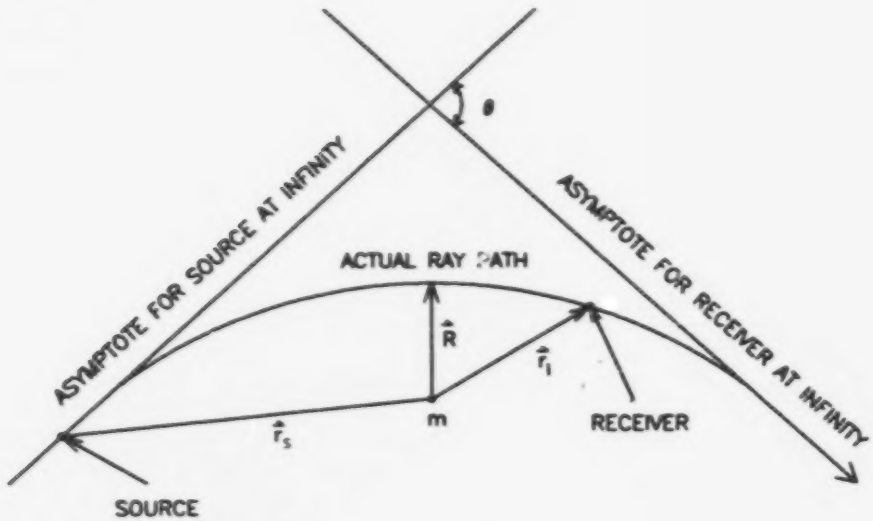

Figure 3. A schematic representation of the geodesic connecting two points in the presence of a gravitational mass

If we further require that $|\mathbf{r}_2 - \mathbf{r}_1|/|\mathbf{r}_1| \to 0$, and make use of

$$\mathbf{r}_2 = \mathbf{r}_1 + \Delta\mathbf{r} \tag{2.21}$$

then:

$$\begin{aligned} r_2 + \hat{\mathbf{r}}_2 \cdot \hat{\mathbf{r}}_s &= r_1\left[1 + 2\,\hat{\mathbf{r}}_1 \cdot \Delta\mathbf{r}/r_1 + (\Delta\mathbf{r}/r_1)^2\right]^{1/2} + \mathbf{r}_1 \cdot \hat{\mathbf{r}}_s + \Delta\mathbf{r} \cdot \hat{\mathbf{r}}_s \\ &\approx r_1\left(1 + \hat{\mathbf{r}}_1 \cdot \Delta\mathbf{r}/r_1\right) + \mathbf{r}_1 \cdot \hat{\mathbf{r}}_s + \Delta\mathbf{r} \cdot \hat{\mathbf{r}}_s \end{aligned} \tag{2.22}$$

In the limit of $\Delta\mathbf{r}/r_1 \to 0$:

$$r_2[1 + \hat{\mathbf{r}}_2 \cdot \hat{\mathbf{r}}_s] \to r_1[1 + \hat{\mathbf{r}}_1 \cdot \hat{\mathbf{r}}_s] + \Delta\mathbf{r} \cdot [\hat{\mathbf{r}}_1 + \hat{\mathbf{r}}_s] \tag{2.23}$$

Substituting into (2.20) and expanding the logarithm, we obtain:

$$\Delta_{Gp} = -\frac{(1+\gamma_{PPN})\mu_p}{c^3} \cdot \frac{[\mathbf{r}_2 - \mathbf{r}_1] \cdot [\hat{\mathbf{r}}_1 + \hat{\mathbf{r}}_s]}{r_1[1 + \hat{\mathbf{r}}_1 \cdot \hat{\mathbf{r}}_s]} \tag{2.24}$$

Using whichever of these three formulations (2.18, 2.20 or 2.24) is computationally appropriate, the model calculates Δ_{Gp} for each of the major bodies in the Solar System (Sun, planets, Earth, and Moon). The total gravitational correction used is:

$$\Delta_G = \sum_{p=1}^{N} \Delta_{Gp} \tag{2.25}$$

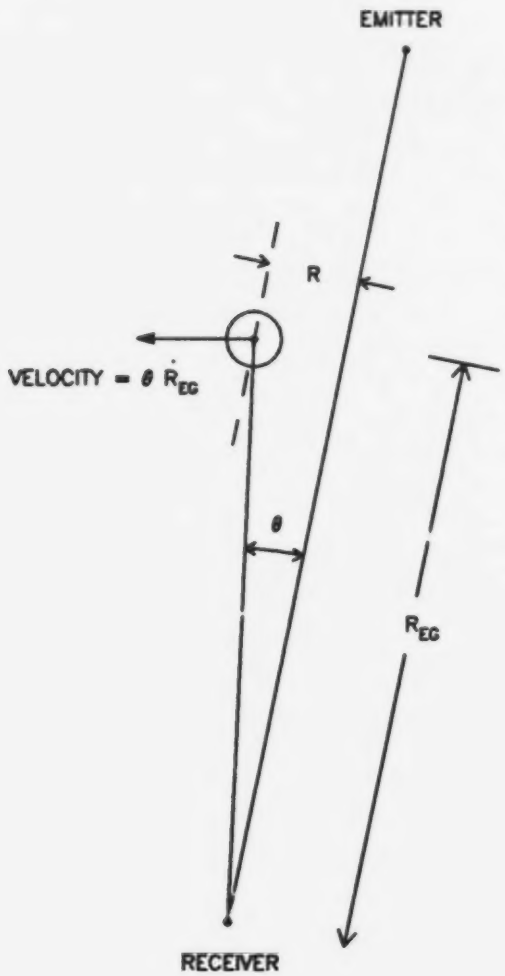

Figure 4. A schematic representation of the motion of a gravitating object during the transit time of a signal from the point of closest approach to reception by an antenna

where the summation to N is over the major bodies in the Solar System. As mentioned above, care must be taken to use the positions of the emitter, the gravitational object, and the receivers at the appropriate times. For a grazing ray emitted by a source at infinity, using the position of the gravitating body G at the time of reception of the signal at station #1 rather than at the time of closest approach of the signal to G can cause a 15-cm error on baselines with a length of one Earth radius as

shown by the following calculation. From figure 4, the calculated distance of closest approach, R, changes during the light transit time, $t_{light\ transit}$, of a signal from a gravitational object at a distance R_{EG} by:

$$\Delta R \approx R_{EG}\dot{\Theta} \cdot t_{light\ transit} = \dot{\Theta} \cdot R_{EG}^2/c \tag{2.26}$$

Since the deflection (see Appendix A) is:

$$\Delta\Theta \approx 2\frac{(1+\gamma_{PPN})\mu_p}{c^3}\left[\frac{c}{R}\right] \tag{2.27}$$

$$\delta(\Delta\Theta) = -\Delta\Theta\left[\frac{\Delta R}{R}\right] = \Delta\Theta\left[\frac{\dot{\Theta}R_{EG}^2}{cR_{EG}\Theta}\right] = \Delta\Theta\left[\frac{R_{EG}}{c\Theta}\right]\frac{\partial\Theta}{\partial t} \tag{2.28}$$

We consider the two bodies of largest mass in the Solar System: the Sun and Jupiter. Their respective deflections $\Delta\Theta$ are 8480 and 73 nanoradians. The angular velocities $\frac{\partial\Theta}{\partial t}$ are estimated to be 6×10^{-11} and 1.7×10^{-8} rad/sec for the Sun and Jupiter. Note that Eq. (2.26) does not apply to the Sun. Its motion in the barycentric frame has a period of 11 years with a radius of the order of the Sun's radius. Using approximate radii and distances from Earth to estimate R_{EG} and Θ, Eq. (2.28) gives 2.5×10^{-8} rad for Jupiter; the corresponding value for the Sun is 7×10^{-11}. For a baseline whose length equals the radius of the Earth, $\delta(\Delta\Theta)R_E$ is thus approximately 0.05 and 15 cm for the Sun and Jupiter, respectively. The effect is much smaller for the Sun in spite of its much larger mass, due to its extremely slow motion in the barycentric frame.

In view of the rapid decrease of gravitational deflection with increasing distance of closest approach, it is extremely unlikely that a situation would arise where a VLBI observation would be close enough to a gravitating body for this correction to be of importance. In order to guard against such an unlikely situation, MASTERFIT code does perform the transit-time correction, however. To obtain the positions of the gravitational objects, we employ an iterative procedure, using the positions and velocities of the objects at signal reception time. If $\mathbf{R}(t_r)$ is the position of the gravitational object at signal reception time, t_r, then that object's position, $\mathbf{R}(t_a)$, at the time, t_a, of closest approach of the ray path to the object was:

$$\mathbf{R}(t_a) = \mathbf{R}(t_r) - \overline{\mathbf{V}}[t_r - t_a] \tag{2.29}$$

$$t_r - t_a = \frac{|\mathbf{R}_c|}{c} \tag{2.30}$$

We do this correction iteratively, using the velocity, $\mathbf{V}(t_r)$, as an approximation of the mean velocity, $\overline{\mathbf{V}}$. Because $v/c \approx 10^{-4}$, an iterative solution:

$$\mathbf{R}_n(t_a) = \mathbf{R}(t_r) - \left[\frac{\mathbf{V}(t_r)}{c}\right]|\mathbf{R}_{n-1}(t_a)| \tag{2.31}$$

rapidly converges to the required accuracy.

Both the gravitational potential effects and the curved wave front effects are calculated independently of each other since the gravitational effects are a small perturbation ($\leq 1''.75$ in angle for Sun-grazing rays, or $\approx$ 9 microradians).

2.2 TIME INFORMATION

Before continuing the description of the geometric model, a few words must be said about time-tag information and the time units which will appear as arguments below. The epoch timing information in the data is taken from the UTC time tags in the data stream at station #1. This time is converted to Terrestrial Dynamic Time (TDT) and is also used as an argument to obtain an *a priori* estimate of Earth orientation. The conversion consists of the following components:

$$TDT = (TDT - TAI) + (TAI - UTC_{BIH}) + (UTC_{BIH} - UTC_0) + (UTC_0 - UTC_1) + UTC_1 \tag{2.32}$$

where in seconds:

$$TDT - TAI = 32.184 \tag{2.33}$$

and where TAI is atomic time. $TAI - UTC_{BIH}$ = published integer second offset after 0^h, January 1, 1972, and

$$TAI - UTC_{BIH} = 9.8922417 + 3.0 \times 10^{-8} \times (UTC_{BIH} - UTC_{0\ BIH}) \tag{2.34}$$

between 0^h, January 1, 1968, and 0^h, January 1, 1972. $UTC_{BIH} - UTC_{0\ BIH}$ = number of UTC seconds relative to January 1, 1972. This is a negative number prior to that date. The software will not allow this quantity to be obtained prior to 1968. $UTC_{BIH} - UTC_0$ = the offset in UTC seconds between BIH UTC and the UTC clock at some secondary standard (usually NBS in Boulder for DSN observations). This can be obtained from BIH Circular D (typical reference is BIH Annual Report, 1981). In practice as of January, 1972, all that we do is use a linear interpolation between $(UTC_{BIH} - UTC_{NBS})$ data points as published in Circular D. The approximation usually is made that the clock at station #1 is very close to the NBS clock, *e.g.*, $UTC_0 - UTC_1 \leq$ 5-10 μs. Since this time is used as epoch time in the observations, the major consequence resulting from an error in this assumption is to make an error in the estimation of UT1−UTC of one second per second of error in $(UTC_i - UTC_j)$. If short baselines are involved, then an error in epoch time causes an error of $\approx B\omega_E \Delta t = 7.3 \times 10^{-6}$ cm per km baseline per μs of clock error. This equals 0.0073 cm of baseline orientation error for a 10-μs clock epoch error on a 100-km baseline.

A priori UT1−UTC and pole positions are normally obtained by interpolation of the BIH Circular D smoothed values. However, any other source of UT1−UTC and pole position could be used provided it is a function of UTC, and is expressed in a left-handed coordinate system (see section 2.6 below). Part of the documentation for any particular set of results should clearly state what were the values of UT1−UTC and pole position used in the data reduction process.

For the Earth model based on the new IAU conventions, the following definitions are employed throughout (Kaplan, 1981):

1. Julian date at epoch J2000 = 2451545.0.
2. All time arguments denoted by T below are measured in Julian centuries of 36525 days of the appropriate time relative to the epoch J2000, *i.e.*, $T = (JD - 2451545.0)/36525$.
3. For the time arguments used to obtain precession, nutation, or to reference the ephemeris, Barycentric Dynamic Time (TDB) is used. This is related to Terrestrial Dynamic Time (TDT) by the following:

$$TDB = TDT + 0.^s001658 \sin(g + 0.0167 \sin(g)) \tag{2.35}$$

where

$$g = \frac{(357.^\circ528 + 35999.^\circ050\ TDT) \times 2\pi}{360^\circ} \tag{2.36}$$

2.3 STATION LOCATION TIME DEPENDENCE

The pre-1984 model considered the three coordinates of station i: r_{sp_i}, λ_i, z_i (radius off spin axis, longitude, and height above the equator, respectively) to be time-invariant. In investigations of tectonic motion, however, a new set of coordinates is usually solved for in the least-squares estimation process for each VLBI session. Post-processing software then makes linear fits to these results to infer bounds on the magnitude of the time rate of change of the station location. Care must be taken that the correlations of coordinates estimated at different epochs are accounted for properly. The advantage of this approach is that the contribution of each session to the overall slope may be independently evaluated, since it is clearly isolated. This procedure is somewhat inconvenient in practice, and an alternative is to introduce the time rates of change of the station coordinates as new parameters in MASTERFIT. The model is linear, with the coordinates at time t expressed as

$$r_{sp_i} = r^0_{sp_i} + \dot{r}_{sp_i}(t - t_0) \tag{2.37}$$

$$\lambda_i = \lambda^0_i + \dot{\lambda}_i(t - t_0) \tag{2.38}$$

$$z_i = z^0_i + \dot{z}_i(t - t_0) \tag{2.39}$$

Here t_0 is a reference epoch, at which the station coordinates are $(r^0_{sp_i}, \lambda^0_i, z^0_i)$.

As an alternative to linear time dependence of the station cylindrical coordinates, the MERIT standard model of tectonic plate rotation is optionally available in MASTERFIT. It is described in an addition to the MERIT standards document (Melbourne et al., 1985), and was denoted AM0-2 in the original paper (Minster and Jordan, 1978). Time dependence of the Cartesian station coordinates is expressed as

$$x_i = x^0_i + (\omega^j_y z^0_i - \omega^j_z y^0_i)(t - t_0) \tag{2.40}$$

$$y_i = y^0_i + (\omega^j_z x^0_i - \omega^j_x z^0_i)(t - t_0) \tag{2.41}$$

$$z_i = z^0_i + (\omega^j_x y^0_i - \omega^j_y x^0_i)(t - t_0) \tag{2.42}$$

where $\omega^j_{x,y,z}$ are velocities of the plate j on which station i resides. Table I gives a list of the rotation rates for the 11 plates in the AM0-2 model.

Table I

Plate Rotation Velocities†: Minster-Jordan AM0-2 Model

Plate	ω_x	ω_y	ω_z
PCFC	-0.12276	0.31163	-0.65537
COCO	-0.63726	-1.33142	0.72556
NAZC	-0.09086	-0.53281	0.63061
CARB	-0.02787	-0.05661	0.10780
SOAM	-0.05604	-0.10672	-0.08642
ANTA	-0.05286	-0.09492	0.21570
INDI	0.43372	0.25011	0.43132
AFRC	0.05660	-0.19249	0.24016
ARAB	0.27885	-0.16744	0.37359
EURA	-0.03071	-0.15865	0.19605
NOAM	0.03299	-0.22828	-0.01427

† units are μdeg/year

At present, there is no facility in MASTERFIT to compute partial derivatives with respect to the plate velocities, or to solve for these quantities.

2.4 TIDAL EFFECTS

As an initial step in calculating the geometric delay, we need to consider the effects of crustal motions on station locations. Among these deformations are solid Earth tides, tectonic motions, and alterations of the Earth's surface due to local geological, hydrological, and atmospheric processes. One possibility is to not model crustal movement other than that due to solid Earth tides, and allow the other effects to manifest themselves as temporal changes of the Earth-fixed baseline. Such a strategy corrupts the estimation of global orientation parameters from a finite set of baselines, and is a known weakness ($\approx$1$-$10 cm/year) of the simplified form of the current model.

In the standard terrestrial coordinate system, tidal effects modify the station location $\mathbf{r}_0$ by an amount

$$\mathbf{\Delta} = \mathbf{\Delta}_{sol} + \mathbf{\Delta}_{ocn} + \mathbf{\Delta}_{atm} + \mathbf{\Delta}_{pol} \tag{2.43}$$

where the four terms are due to solid Earth tides, ocean loading, atmosphere loading, and pole tide, respectively. Other Earth-fixed effects would be incorporated by augmenting the definition of $\mathbf{\Delta}$.

2.4.1 Solid Earth Tides

Alteration of the positions of the stations by solid Earth tides is rather complicated due to their coupling with the ocean tides, and the effects of local geology. We have chosen to gloss over these complications initially, and to incorporate the simple quadrupole response model described by J. G. Williams (1970), who used Melchior (1966) as a reference. Let $\mathbf{r}_t$ be the Cartesian coordinates of a station in a geocentric frame (x axis vertical, y axis eastward, and the z axis northward) on a spherical Earth. Further, let $\mathbf{R}_s$ be the position of a perturbing source in the terrestrial reference system, and $\mathbf{r}_0$ the station position in the same coordinates. If h and l are the Love numbers, ψ a phase shift of the tidal effects, and $\mathbf{r}_p$ the phase-shifted station location in the terrestrial system, then the tidal displacements are

$$\delta = \sum_s [h g_{1s},\ l g_{2s},\ l g_{3s}]^T \tag{2.44}$$

where

$$g_{1s} = \frac{3\mu_s r_p^2}{R_s^5}\left[\frac{[\mathbf{r}_p \cdot \mathbf{R}_s]^2}{2} - \frac{r_p^2 R_s^2}{6}\right] \tag{2.45}$$

$$g_{2s} = \frac{3\mu_s r_p^2}{R_s^5}[\mathbf{r}_p \cdot \mathbf{R}_s][Y_s x_p - X_s y_p]\frac{|\mathbf{r}_p|}{\sqrt{x_p^2 + y_p^2}} \tag{2.46}$$

$$g_{3s} = \frac{3\mu_s r_p^2}{R_s^5}[\mathbf{r}_p \cdot \mathbf{R}_s]\left[\sqrt{x_p^2 + y_p^2}\ Z_s - \frac{z_p}{\sqrt{x_p^2 + y_p^2}}[x_p X_s + y_p Y_s]\right] \tag{2.47}$$

μ_s is the ratio of the mass of the disturbing object, s, to the mass of the Earth, and

$$\mathbf{R}_s = [X_s, Y_s, Z_s]^T \tag{2.48}$$

is the vector from the center of the Earth to that body. The summation is over all tide-producing bodies, of which we include only the Sun and the Moon. If the tidal effect at time t_1 is desired, the position of the tide-producing mass at time

$$t_1 - \delta t = t_1 - |\mathbf{R}(t_1 - \delta t)|/c \tag{2.49}$$

should be used (a nuance we have not yet incorporated).

The phase-shifted station vector above is calculated employing a phase lag, or equivalently, employing a right-handed rotation, L, through an angle ψ about the z axis of date, $\mathbf{r}_p = L\mathbf{r}_0$. This lag matrix, L, is:

$$L = \begin{pmatrix} \cos\psi & \sin\psi & 0 \\ -\sin\psi & \cos\psi & 0 \\ 0 & 0 & 1 \end{pmatrix} \tag{2.50}$$

By a positive value of ψ we mean that the peak response on an Earth meridian occurs at a time $\delta t = \psi/\omega_E$ after that meridian containing $\mathbf{r}_0$ crosses the tide-producing object, where ω_E is the angular rotation rate of the Earth. In the vertical component, the peak response occurs when the meridian containing $\mathbf{r}_p$ also includes $\mathbf{r}_s$. The difference between geodetic and geocentric latitude can affect this model on the order of the (tidal effect)/(flattening factor) $\approx$ 0.1 cm.

To convert this locally referenced strain, δ, to the Earth-fixed frame, two additional rotations must be performed. The first, W, rotates by an angle, $-\phi_s$, about the y axis to an equatorial system. The second, V, rotates about the resultant z axis by angle, $-\lambda_s$, to bring the displacements into the standard geocentric coordinate system. The result is

$$\Delta_{xyz} = VW\delta \tag{2.51}$$

where

$$W = \begin{pmatrix} \cos\phi_s & 0 & -\sin\phi_s \\ 0 & 1 & 0 \\ \sin\phi_s & 0 & \cos\phi_s \end{pmatrix} \tag{2.52}$$

and

$$V = \begin{pmatrix} \cos\lambda_s & -\sin\lambda_s & 0 \\ \sin\lambda_s & \cos\lambda_s & 0 \\ 0 & 0 & 1 \end{pmatrix} \tag{2.53}$$

Actually, the product of these two matrices is coded:

$$VW = \begin{pmatrix} \cos\lambda_s\cos\phi_s & -\sin\lambda_s & -\cos\lambda_s\sin\phi_s \\ \sin\lambda_s\cos\phi_s & \cos\lambda_s & -\sin\lambda_s\sin\phi_s \\ \sin\phi_s & 0 & \cos\phi_s \end{pmatrix} \tag{2.54}$$

2.4.2 Ocean Loading

This section is concerned with secondary tidal effects, i.e., the elastic response of the Earth's crust to ocean tides, which move the observing stations to the extent of a few cm. Such effects are commonly labeled "ocean loading." The most complete recent model appears to be that described by Pagiatakis (1982) and by Pagiatakis, Langley, and Vanicek (1982), which is implemented as an option in the current MASTERFIT. The formulation and coding are general enough, however, to permit other inputs to be used in place of the Pagiatakis ocean loading model. Because the station motions caused by response to ocean tides appear to be limited to approximately 3 cm for sites well removed from the coast, no estimation capability was deemed necessary at present. This decision is supported by the fact that for locations near the coast, where the effects may be more sizable, and which would thus be expected to produce data useful in parameter estimation, the elastic response modeling is as yet inadequate (Agnew, 1982). As suggested in section 8 of the initial version of this report (V1.0), local Earth motion can be partially accounted for by varying the Love numbers for each station. The present model entails deriving an expression for the locally referenced displacement δ due to ocean loading. In the vertical, N-S, E-W local coordinate system at time t,

$$\delta_j = \sum_{i=1}^{N} \xi_i^j \cos(\omega_i t + V_i - \delta_i^j) \tag{2.55}$$

The quantities ω_i (frequency of tidal constituent i) and V_i (astronomical argument of constituent i) depend only on the ephemeris information (positions of the Sun and Moon). On the other hand the amplitude ξ_i^j and Greenwich phase lag δ_i^j of each tidal component j are determined by the particular model assumed for the deformation of the Earth. As of December 1984, software for calculating these deformations at an arbitrary point on the Earth's surface exists at JPL only for the Pagiatakis-Langley model. Six tidal components are included [$N = 6$ in Eq. (2.55)]: the M_2, S_2, K_1, O_1, N_2, and P_1 tides,

all of which have periods close to either 12 or 24 hours. The local displacement vector is transformed via Eqs. (2.54) and (2.51) to the displacement Δ_{ocn} in the standard geocentric frame.

Input to MASTERFIT provides for specification of an arbitrary number of frequencies and astronomical arguments ω_i and V_i, followed by tables of the local distortions and their phases, ξ_i^j and δ_i^j, calculated from the ocean tidal loading model of choice. In particular, longer-period tidal constituents can be accommodated in this fashion.

There are presently four choices of models. As mentioned above, the six components of the Pagiatakis-Langley model can be calculated by separate software for an arbitrarily located station to generate input tables for MASTERFIT. This has been done for all stations commonly employed in JPL VLBI experiments. There is no comparable facility to obtain amplitudes and phases for the Agnew (1982), Scherneck (1983), or Goad (1983) models. Consequently, for these three models, MASTERFIT input tables only exist for the limited set of stations considered by these authors. Agnew considers only five components (omitting P_1), while Scherneck includes five components in addition to the Pagiatakis-Langley set: K_2, Q_1, M_f, M_m, and S_{sa}. These all have amplitudes of 1 mm or smaller and, thus, are not expected to be significant at the present level of VLBI experimental accuracy. Goad's MERIT standard model only specifies vertical displacements, but includes three components (K_2, Q_1 and M_f) in addition to Pagiatakis-Langley. Due to their bulk, none of the tables of tidal amplitudes is reproduced here, but are available on request in computer-readable form. The default tidal model in MASTERFIT remains the Williams quadrupole solid Earth tide model with no ocean loading.

2.4.3 Atmosphere Loading

By analogy with the consequences of ocean tides that were considered in the previous section, a time-varying atmospheric pressure distribution can induce crustal deformation. A recent paper by Rabbel and Schuh (1986) estimates the effects of atmospheric loading on VLBI baseline determinations, and concludes that they may amount to many millimeters of seasonal variation. In contrast to ocean tidal effects, analysis of the situation in the atmospheric case does not benefit from the presence of a well-understood periodic driving force. Otherwise, estimation of atmospheric loading via Green's function techniques is analogous to methods used to calculate ocean loading effects. Rabbel and Schuh recommend a simplified form of the dependence of the vertical crust displacement on pressure distribution. It involves only the instantaneous pressure at the site in question, and an average pressure over a circular region C of radius $R = 2000$ km surrounding the site. The expression for the vertical displacement (mm) is:

$$\Delta r = -0.35p - 0.55\bar{p} \tag{2.56}$$

where p is the local pressure anomaly, and $\bar{p}$ the pressure anomaly within the 2000-km circular region mentioned above (both quantities are in mbar). Note that the reference point for this displacement is the site location at standard pressure (1013.3 mbar). The locally referenced Δr is transformed to the standard geocentric coordinate system via the transformation (2.54).

It was decided to incorporate this rudimentary model into MASTERFIT as an optional part of the model, with an additional mechanism for characterising $\bar{p}$. The two-dimensional surface pressure distribution surrounding a site is described by

$$p(x,y) = A_0 + A_1 x + A_2 y + A_3 x^2 + A_4 xy + A_5 y^2 \tag{2.57}$$

where x and y are the local East and North distances of the point in question from the VLBI site. The pressure anomaly $\bar{p}$ may then be evaluated by the simple integration

$$\bar{p} = \iint_C dx\,dy\; p(x,y) \Big/ \iint_C dx\,dy \tag{2.58}$$

giving

$$\bar{p} = A_0 + (A_3 + A_5)R^2/4 \tag{2.59}$$

It remains the task of the data analyst to perform a quadratic fit to the available weather data to determine the coefficients A_{0-5}. Future advances in understanding the atmosphere-crust elastic interaction can probably be accommodated by adjusting the coefficients in Eq. (2.56).

2.4.4 Pole Tide

In addition to the effects of ocean tides and atmospheric pressure variations, another secondary tidal effect is the displacement of a station by the elastic response of the Earth's crust to shifts in the spin axis orientation. The spin axis is known to describe a circle of $\approx$ 20-m diameter at the north pole. Depending on where the spin axis pierces the crust at the instant of a VLBI measurement, the "pole tide" displacement will vary from time to time. This effect must be included if centimeter accuracy is desired.

Yoder (1984) derived an expression for the displacement of a point at latitude ϕ, longitude λ due to the pole tide:

$$\begin{aligned}\boldsymbol{\delta} = -\frac{\omega_E^2 R}{g}\big[&\sin\phi\cos\phi(x\cos\lambda + y\sin\lambda)h\hat{\mathbf{r}} \\ &+ \cos 2\phi(x\cos\lambda + y\sin\lambda)l\hat{\boldsymbol{\phi}} \\ &+ \sin\phi(-x\sin\lambda + y\cos\lambda)l\hat{\boldsymbol{\lambda}}\big]\end{aligned} \tag{2.60}$$

Here ω_E is the rotation rate of the Earth, R the radius of the (spherical) Earth, g the acceleration due to gravity at the Earth's surface, and h and l the customary Love numbers. Displacements of the spin axis from the 1903.0 CIO pole position along the x and y axes are given by x and y. Eq. (2.60) shows how these map into station displacements along the unit vectors in the radial ($\hat{\mathbf{r}}$), latitude ($\hat{\boldsymbol{\phi}}$), and longitude ($\hat{\boldsymbol{\lambda}}$) directions. With the standard values $\omega_E = 7.292 \times 10^{-5}$ rad/sec, $R = 6378$ km, and $g = 980.665$ g/cm^2, the factor $\omega_E^2 R/g = 3.459 \times 10^{-3}$. Since the maximum values of x and y are of the order of 10 meters, and $h \approx 0.6$, $l \approx 0.08$, the maximum displacement due to the pole tide is 1 to 2 cm, depending on the location of the station (ϕ, λ).

As in the case of the previously considered tidal effects, the locally referenced displacement $\boldsymbol{\delta}$ is transformed via the transformation (2.54) to give the displacement $\boldsymbol{\Delta}_{pol}$ in the standard geocentric coordinate system. The pole tide effect has been coded as an optional part of the MASTERFIT model. It is only applied if specifically requested, *i.e.*, the default model contains no pole tide contributions to the station locations.

After each of the locally referenced tidal displacements has been transformed to standard terrestrial coordinates, the station location is

$$\mathbf{r}_t = \mathbf{r}_0 + \boldsymbol{\Delta}_{sol} + \boldsymbol{\Delta}_{ocn} + \boldsymbol{\Delta}_{atm} + \boldsymbol{\Delta}_{pol} \tag{2.61}$$

2.5 TRANSFORMATION FROM TERRESTRIAL TO CELESTIAL COORDINATE SYSTEMS

The Earth is approximately an oblate spheroid, spinning in the presence of two massive moving objects (the Sun and the Moon) which are positioned such that their time-varying gravitational effects not only produce tides on the Earth, but also subject it to torques. In addition, the Earth is covered by a complicated fluid layer, and also is not perfectly solid internally. As a result, the orientation of the Earth is a very complicated function of time, which to first order can be represented as the composite of a time-varying rotation rate, a wobble, a nutation, and a precession. The exchange of angular momentum between the solid Earth and the fluids on its surface is not readily predictable, and thus must be continually determined experimentally. Nutation and precession are well modeled theoretically. However, at the accuracy with which VLBI can determine baseline vectors, even these models are not completely adequate.

Currently, the rotational transformation, Q, of coordinate frames from the terrestrial frame to the celestial geocentric frame is composed of 6 separate rotations (actually 10, since the nutation transformation, N, consists of 3 transformations in itself, as does the "perturbation" transformation, Ω) applied to a vector in the terrestrial system:

$$Q = \Omega PNUXY \tag{2.62}$$

Thus, if $\mathbf{r}_t$ is a station location expressed in the terrestrial system, *e.g.*, the result of (2.61), that location, $\mathbf{r}_c$, expressed in the celestial system is

$$\mathbf{r}_c = Q\mathbf{r}_t \tag{2.63}$$

This particular formulation follows the historical path of astrometry, and is couched in that language. While aesthetically unsatisfactory with modern measurement techniques, such a formulation is currently practical for intercomparison of techniques and for effecting a smooth inclusion of the interferometer data into the long historical record of astrometric data. Much more pleasing aesthetically would be the separation of Q into two rotation matrices:

$$Q = Q_1 Q_2 \tag{2.64}$$

where Q_2 are those rotations to which the Earth would be subjected if all external torques were removed (approximately UXY above), and where Q_1 are those rotations arising from external torques (approximately ΩPN above). Even then, the tidal response of the Earth prevents such a separation from being perfectly realized. Eventually, the entire problem of obtaining the matrix Q, and the tidal effects on station locations should be done numerically. Note that since we rotate the Earth rather than the celestial sphere, our rotation matrices, Ω, P, and N, will be the transposes of those used to rotate the celestial system of J2000 to a celestial system of date.

2.6 UT1 AND POLAR MOTION

The first transformation, Y, is a right-handed rotation about the x axis of the terrestrial frame by an angle Θ_2. Currently, the terrestrial frame is the 1903.0 CIO frame, except that the positive y axis is at 90 degrees east (Moscow). The x axis is coincident with the 1903.0 meridian of Greenwich, and the z axis is the 1903.0 standard pole.

$$Y = \begin{pmatrix} 1 & 0 & 0 \\ 0 & \cos\Theta_2 & \sin\Theta_2 \\ 0 & -\sin\Theta_2 & \cos\Theta_2 \end{pmatrix} \tag{2.65}$$

where Θ_2 is identical to the Θ_y that may be readily obtained from the pole position published by BIH.

The next rotation in sequence is the right-hand rotation through an angle Θ_1 about the y axis obtained after the previous rotation has been applied:

$$X = \begin{pmatrix} \cos\Theta_1 & 0 & -\sin\Theta_1 \\ 0 & 1 & 0 \\ \sin\Theta_1 & 0 & \cos\Theta_1 \end{pmatrix} \tag{2.66}$$

In this rotation, Θ_1 is identical to the Θ_x obtainable from the BIH value for the pole position. Note that we have incorporated in the matrix definitions the transformation from the left-handed system used by BIH to the right-handed system we use. Note also that instead of BIH data used as a pole definition, we could instead use any other source of polar motion data provided it was represented in a left-handed system. The only effect would be a change in the definition of the terrestrial reference system.

The application of "XY" to a vector in the terrestrial system of coordinates expresses that vector as it would be observed in a coordinate frame whose z axis was along the Earth's ephemeris pole. The third rotation, U, is about the resultant z axis obtained by applying "XY". It is a rotation through the angle, $-H$, where H is the hour angle of the true equinox of date (i.e., the dihedral angle measured westward between the xz plane defined above and the meridian plane containing the true equinox of date). The equinox of date is the point defined on the celestial equator by the intersection of the mean ecliptic with that equator. It is that intersection where the mean ecliptic rises from below the equator to above it (ascending node).

$$U = \begin{pmatrix} \cos H & -\sin H & 0 \\ \sin H & \cos H & 0 \\ 0 & 0 & 1 \end{pmatrix} \tag{2.67}$$

This angle H is composed of two parts:

$$H = h_\gamma + \alpha_E \tag{2.68}$$

where h_γ is the hour angle of the mean equinox of date, and α_E is the difference in hour angle of the true equinox of date and the mean equinox of date, a difference which is due to the nutation of the Earth. This set of definitions is cumbersome and couples the nutation and precession effects into Earth rotation measurements. However, in order to provide a direct estimate of conventional $UT1$ it is convenient to endure this historical approach, at least for the near future.

$UT1$ (universal time) is defined to be such that the hour angle of the mean equinox of date is given by the following expression (Aoki et al., 1982, and Kaplan, 1981):

$$\begin{aligned} h_\gamma = UT1 + 6^h\ 41^m\ 50^s.54841 + 8640184^s.812866\ T_u \\ + 0^s.093104\ T_u^2 - 6^s.2 \times 10^{-6}\ T_u^3 \end{aligned} \tag{2.69}$$

where

$$T_u = \frac{(\text{Julian } UT1 \text{ date}) \ - \ 2451545.0}{36525} \tag{2.70}$$

The actual equivalent expression which is coded is:

$$\begin{aligned} h_\gamma = & 2\pi(UT1 \text{ Julian day fraction}) + 67310^s.54841 \\ & + 8640184^s.812866\ T_u + 0^s.093104\ T_u^2 - 6^s.2 \times 10^{-6}\ T_u^3 \end{aligned} \tag{2.71}$$

This expression produces a time, $UT1$, which tracks the Greenwich hour angle of the real Sun to within 16^m. However, it really is sidereal time, modified to fit our intuitive desire to have the Sun directly overhead at noon on the Greenwich meridian. Historically, differences of $UT1$ from a uniform measure of time, such as atomic time, have been used in specifying the orientation of the Earth. Note that this definition has buried in it the precession constant since it refers to the mean equinox of date.

By the very definition of "mean of date" and "true of date", nutation causes a difference in the hour angles of the mean equinox of date and the true equinox of date. This difference, called the "equation of equinoxes", is denoted by α_E and is obtained accordingly:

$$\alpha_E = \tan^{-1}\left(\frac{y_{\gamma'}}{x_{\gamma'}}\right) = \tan^{-1}\left(\frac{N_{21}^{-1}}{N_{11}^{-1}}\right) = \tan^{-1}\left(\frac{N_{12}}{N_{11}}\right) \tag{2.72}$$

where th vector

$$\begin{pmatrix} x'_\gamma \\ y'_\gamma \\ z'_\gamma \end{pmatrix} = N_{ij}^{-1}\begin{pmatrix} 1 \\ 0 \\ 0 \end{pmatrix} \tag{2.73}$$

is the unit vector, in true equatorial coordinates of date, toward the mean equinox of date. In mean equatorial coordinates of date, this same unit vector is just $(1,0,0)^T$. The matrix N_{ij}^{-1} is just the inverse (or equally, the transpose) of the transformation matrix N which will be defined below to effect the transformation from true equatorial coordinates of date to mean equatorial coordinates of date.

Depending on the smoothing used to produce the *a priori* $UT1 - UTC$ series, the short-period (t < 35 days) fluctuations in $UT1$ due to changes in the latitude and size of the mean tidal bulge may or may not be smoothed out. Since we want as accurate an *a priori* as possible, it may be necessary to add this effect to the $UT1$ *a priori* obtained from the series, $UT1_{smoothed}$. If this option is selected, then the desired *a priori* $UT1$ is given by

$$UT1_{a\ priori} = UT1_{smoothed} + \Delta UT1 \tag{2.74}$$

$UT1_{smoothed}$ represents an appropriately smoothed *a priori* measurement of the orientation of the Earth (*i.e.*, typically BIH Circular D smoothed or, even better, $UT1R$), for which the short period (t < 35 days) tidal effects have either been averaged to zero, or, as in the case of $UT1R$, removed before smoothing. This $\Delta UT1$ can be represented as

$$\Delta UT1 = \sum_{i=1}^{N}\left[A_i \sin\left[\sum_{j=1}^{5} k_{ij}\alpha_j\right]\right] \tag{2.75}$$

where N is chosen to include all terms with a period less than 35 days. There are no other contributions until a period of 90 days is reached. However, these long-period terms are included by the measurements of the current Earth-orientation measurement services. The values for k_{ij} and A_i, along with the period involved, are given in Table II. The α_i for $i = 1, 5$ are just the angles defined below in the nutation series as l, l', F, D, and Ω, respectively. In Table II, the sign of the 14.73 day term has been changed from that published [Yoder (1982)] to remove a sign error in the article referenced. Otherwise, the values in Table II are those given by BIH (1982) as derived from Yoder et al. (1981).

It might be appropriate at this point to describe the interpolation method used in MASTERFIT to obtain *a priori* polar motion and $UT1$ values. These are normally available as tables at 5-day intervals, from either BIH or the IRIS project (IAG, 1986). Linear interpolation is performed for all three quantities. If the short-period tidal terms $\Delta UT1$ are present in the tabular values, they are subtracted before interpolation, and added back to the final value. With the present accuracy of determinations of pole position and $UT1$, linear interpolation over a 5-day interval may be inadequate, possibly giving rise to 0.1 to 0.2 ms errors in $UT1$. Quadratic spline interpolation is being considered as an alternative. Even with the present code, however, the highest possible accuracy may be achieved by performing the interpolation externally to MASTERFIT, and supplying it with tables of values more closely spaced in time for the final internal linear interpolation. The Kalman-filtered UTPM values of Eubanks et al. (1984) are ideally suited for this purpose.

Table II
Periodic Tidally Induced Variations in UT1
with Periods Less than 35 Days

Index i	Period (days)	Argument coefficient k_{i1}	k_{i2}	k_{i3}	k_{i4}	k_{i5}	A_i (0".0001)
1	5.64	1	0	2	2	2	-0.02
2	6.85	2	0	2	0	1	-0.04
3	6.86	2	0	2	0	2	-0.10
4	7.09	0	0	2	2	1	-0.05
5	7.10	0	0	2	2	2	-0.12
6	9.11	1	0	2	0	0	-0.04
7	9.12	1	0	2	0	1	-0.41
8	9.13	1	0	2	0	2	-0.99
9	9.18	3	0	0	0	0	-0.02
10	9.54	-1	0	2	2	1	-0.08
11	9.56	-1	0	2	2	2	-0.20
12	9.61	1	0	0	2	0	-0.08
13	12.81	2	0	2	-2	2	0.02
14	13.17	0	1	2	0	2	0.03
15	13.61	0	0	2	0	0	-0.30
16	13.63	0	0	2	0	1	-3.21
17	13.66	0	0	2	0	2	-7.76
18	13.75	2	0	0	0	-1	0.02
19	13.78	2	0	0	0	0	-0.34
20	13.81	2	0	0	0	1	0.02
21	14.19	0	-1	2	0	2	-0.02
22	14.73	0	0	0	2	-1	0.05
23	14.77	0	0	0	2	0	-0.73
24	14.80	0	0	0	2	1	-0.05
25	15.39	0	-1	0	2	0	-0.05
26	23.86	1	0	2	-2	1	0.05
27	23.94	1	0	2	-2	2	0.10
28	25.62	1	1	0	0	0	0.04
29	26.88	-1	0	2	0	0	0.05
30	26.98	-1	0	2	0	1	0.18
31	27.09	-1	0	2	0	2	0.44
32	27.44	1	0	0	0	-1	0.53
33	27.56	1	0	0	0	0	-8.26
34	27.67	1	0	0	0	1	0.54
35	29.53	0	0	0	1	0	0.05
36	29.80	1	-1	0	0	0	-0.06
37	31.66	-1	0	0	2	-1	0.12
38	31.81	-1	0	0	2	0	-1.82
39	31.96	-1	0	0	2	1	0.13
40	32.61	1	0	-2	2	-1	0.02
41	34.85	-1	-1	0	2	0	-0.09

It is convenient to apply "UXY" as a group. To parts in 10^{12}, $XY = YX$. However, with the same accuracy $UXY \neq XYU$. Neglecting terms of $O(\Theta^2)$ (which produce station location errors of approximately 6×10^{-6} meters):

$$UXY = \begin{pmatrix} \cos H & -\sin H & -\sin\Theta_1 \cos H - \sin\Theta_2 \sin H \\ \sin H & \cos H & -\sin\Theta_1 \sin H + \sin\Theta_2 \cos H \\ \sin\Theta_1 & -\sin\Theta_2 & 1 \end{pmatrix} \tag{2.76}$$

2.7 NUTATION

With the completion of the $UT1$ and polar motion transformations, we are left with a station location vector, $\mathbf{r}_{date}$. This is the station location relative to true equatorial celestial coordinates of date. The last set of transformations are nutation, N, precession, P, and the perturbation rotation, Ω, applied in that order. These transformations give the station location, $\mathbf{r}_c$, in celestial equatorial coordinates:

$$\mathbf{r}_c = \Omega P N \mathbf{r}_{date} \tag{2.77}$$

The transformation matrix N is a composite of three separate rotations (Melbourne et al., 1968):

1. $\mathbf{A}(\varepsilon)$: true equatorial coordinates of date to ecliptic coordinates of date.

$$A(\varepsilon) = \begin{pmatrix} 1 & 0 & 0 \\ 0 & \cos\varepsilon & \sin\varepsilon \\ 0 & -\sin\varepsilon & \cos\varepsilon \end{pmatrix} \tag{2.78}$$

2. $C^T(\delta\psi)$: nutation in longitude from ecliptic coordinates of date to mean ecliptic coordinates of date.

$$C^T(\delta\psi) = \begin{pmatrix} \cos\delta\psi & \sin\delta\psi & 0 \\ -\sin\delta\psi & \cos\delta\psi & 0 \\ 0 & 0 & 1 \end{pmatrix} \tag{2.79}$$

where $\delta\psi$ is the nutation in ecliptic longitude.

3. $A^T(\bar{\varepsilon})$: ecliptic coordinates of date to mean equatorial coordinates.

In ecliptic coordinates of date, the mean equinox is at an angle $\delta\psi = \tan^{-1}(y_{\bar{\gamma}}/x_{\bar{\gamma}})$. $\delta\varepsilon = \varepsilon - \bar{\varepsilon}$ is the nutation in obliquity, and $\bar{\varepsilon}$ is the mean obliquity (the dihedral angle between the plane of the ecliptic and the mean plane of the equator). "Mean" as used in this section implies that the short-period ($T \leq 18.6$ years) effects of nutation have been removed. Actually, the separation between nutation and precession is rather arbitrary, but historical. The composite rotation is:

$$N = A^T(\bar{\varepsilon}) C^T(\delta\psi) A(\varepsilon) \tag{2.80}$$

$$= \begin{pmatrix} \cos\delta\psi & \cos\varepsilon\sin\delta\psi & \sin\varepsilon\sin\delta\psi \\ -\cos\bar{\varepsilon}\sin\delta\psi & \cos\bar{\varepsilon}\cos\varepsilon\cos\delta\psi + \sin\bar{\varepsilon}\sin\varepsilon & \cos\bar{\varepsilon}\sin\varepsilon\cos\delta\psi - \sin\bar{\varepsilon}\cos\varepsilon \\ -\sin\bar{\varepsilon}\sin\delta\psi & \sin\bar{\varepsilon}\cos\varepsilon\cos\delta\psi - \cos\bar{\varepsilon}\sin\varepsilon & \sin\bar{\varepsilon}\sin\varepsilon\cos\delta\psi + \cos\bar{\varepsilon}\cos\varepsilon \end{pmatrix}$$

The 1980 IAU nutation model (Seidelmann, 1982, and Kaplan, 1981) is used to obtain the values for $\delta\psi$ and $\varepsilon - \bar{\varepsilon}$. The mean obliquity is obtained from Lieske et al. (1977) or from Kaplan (1981):

$$\bar{\varepsilon} = 23^\circ\ 26'\ 21.''448 - 46.''8150\,T - 5.''9 \times 10^{-4} T^2 + 1.''813 \times 10^{-3} T^3 \tag{2.81}$$

This nutation in longitude ($\delta\psi$) and in obliquity ($\delta\varepsilon = \varepsilon - \bar{\varepsilon}$) can be represented by a series expansion of the sines and cosines of linear combinations of five fundamental arguments. These are (Kaplan, 1981, Cannon, 1981):

1. the mean anomaly of the Moon:

$$\alpha_1 = l = 485866''.733 + (1325^r + 715922''.633)\,T + 31''.310\,T^2 + 0''.064\,T^3 \tag{2.82}$$

2. the mean anomaly of the Sun:

$$\alpha_2 = l' = 1287099''.804 + (99^r + 1292581''.224)\,T - 0''.577\,T^2 - 0.''012\,T^3 \tag{2.83}$$

3. the mean argument of latitude of the Moon:

$$\alpha_3 = F = 335778''.877 + (1342^r + 295263''.137)\,T - 13''.257\,T^2 + 0''.011\,T^3 \tag{2.84}$$

4. the mean elongation of the Moon from the Sun:

$$\alpha_4 = D = 1072261''.307 + (1236^r + 1105601''.328)\,T - 6''.891\,T^2 + 0''.019\,T^3 \tag{2.85}$$

5. the mean longitude of the ascending lunar node:

$$\alpha_5 = \Omega = 450160''.280 - (5^r + 482890''.539)\,T + 7''.455\,T^2 + 0''.008\,T^3 \tag{2.86}$$

where $1^r = 360° = 1296000''$.

With these fundamental arguments, the nutation quantities then can be represented by

$$\delta\psi = \sum_{j=1}^{N}\left[(A_{0j} + A_{1j}T)\sin\left[\sum_{i=1}^{5} k_{ji}\alpha_i(T)\right]\right] \tag{2.87}$$

and

$$\delta\varepsilon = \sum_{j=1}^{N}\left[(B_{0j} + B_{1j}T)\cos\left[\sum_{i=1}^{5} k_{ji}\alpha_i(T)\right]\right] \tag{2.88}$$

where the various values of α_i, k_{ji}, A_j, and B_j are tabulated in Table III.

An additional set of terms can be optionally added to the nutations $\delta\psi$ and $\delta\varepsilon$ in Eqs. (2.87) and (2.88). These include the out-of-phase nutations, and the free-core nutations (Yoder, 1983) with period ω_f (nominally 460 days). The "nutation tweaks" $\Delta\psi$ and $\Delta\varepsilon$ are arbitrary constant increments of the nutation angles $\delta\psi$ and $\delta\varepsilon$. Unlike the usual nutation expressions, they have no time dependence. The out-of-phase nutations, which are not included in the IAU 1980 nutation series, are identical to Eqs. (2.87) and (2.88), with the replacements sin $\leftrightarrow$ cos:

$$\delta\psi = \sum_{j=1}^{N}\left[(A_{2j} + A_{3j}T)\cos\left[\sum_{i=1}^{5} k_{ji}\alpha_i(T)\right]\right] \tag{2.89}$$

and

$$\delta\varepsilon = \sum_{j=1}^{N}\left[(B_{2j} + B_{3j}T)\sin\left[\sum_{i=1}^{5} k_{ji}\alpha_i(T)\right]\right] \tag{2.90}$$

Table III

1980 IAU Theory of Nutation

Index j	Period (days)	Argument coefficient k_{j1}	k_{j2}	k_{j3}	k_{j4}	k_{j5}	A_{0j} (0".0001)	A_{1j}	B_{0j} (0".0001)	B_{1j}
1	6798.4	0	0	0	0	1	-171996	-174.2	92025	8.9
2	3399.2	0	0	0	0	2	2062	0.2	-895	0.5
3	1305.5	-2	0	2	0	1	46	0.0	-24	0.0
4	1095.2	2	0	-2	0	0	11	0.0	0	0.0
5	1615.7	-2	0	2	0	2	-3	0.0	1	0.0
6	3232.9	1	-1	0	-1	0	-3	0.0	0	0.0
7	6786.3	0	-2	2	-2	1	-2	0.0	1	0.0
8	943.2	2	0	-2	0	1	1	0.0	0	0.0
9	182.6	0	0	2	-2	2	-13187	-1.6	5736	-3.1
10	365.3	0	1	0	0	0	1426	-3.4	54	-0.1
11	121.7	0	1	2	-2	2	-517	1.2	224	-0.6
12	365.2	0	-1	2	-2	2	217	-0.5	-95	0.3
13	177.8	0	0	2	-2	1	129	0.1	-70	0.0
14	205.9	2	0	0	-2	0	48	0.0	1	0.0
15	173.3	0	0	2	-2	0	-22	0.0	0	0.0
16	182.6	0	2	0	0	0	17	-0.1	0	0.0
17	386.0	0	1	0	0	1	-15	0.0	9	0.0
18	91.3	0	2	2	-2	2	-16	0.1	7	0.0
19	346.6	0	-1	0	0	1	-12	0.0	6	0.0
20	199.8	-2	0	0	2	1	-6	0.0	3	0.0
21	346.6	0	-1	2	-2	1	-5	0.0	3	0.0
22	212.3	2	0	0	-2	1	4	0.0	-2	0.0
23	119.6	0	1	2	-2	1	4	0.0	-2	0.0
24	411.8	1	0	0	-1	0	-4	0.0	0	0.0
25	131.7	2	1	0	-2	0	1	0.0	0	0.0
26	169.0	0	0	-2	2	1	1	0.0	0	0.0
27	329.8	0	1	-2	2	0	-1	0.0	0	0.0
28	409.2	0	1	0	0	2	1	0.0	0	0.0
29	388.3	-1	0	0	1	1	1	0.0	0	0.0
30	117.5	0	1	2	-2	0	-1	0.0	0	0.0
31	13.7	0	0	2	0	2	-2274	-0.2	977	-0.5
32	27.6	1	0	0	0	0	712	0.1	-7	0.0
33	13.6	0	0	2	0	1	-386	-0.4	200	0.0
34	9.1	1	0	2	0	2	-301	0.0	129	-0.1
35	31.8	1	0	0	-2	0	-158	0.0	-1	0.0
36	27.1	-1	0	2	0	2	123	0.0	-53	0.0
37	14.8	0	0	0	2	0	63	0.0	-2	0.0
38	27.7	1	0	0	0	1	63	0.1	-33	0.0
39	27.4	-1	0	0	0	1	-58	-0.1	32	0.0
40	9.6	-1	0	2	2	2	-59	0.0	26	0.0

Table III cont.

1980 IAU Theory of Nutation

Index j	Period (days)	Argument coefficient k_{j1}	k_{j2}	k_{j3}	k_{j4}	k_{j5}	A_{0j} (0".0001)	A_{1j}	B_{0j} (0".0001)	B_{1j}
41	9.1	1	0	2	0	1	-51	0.0	27	0.0
42	7.1	0	0	2	2	2	-38	0.0	16	0.0
43	13.8	2	0	0	0	0	29	0.0	-1	0.0
44	23.9	1	0	2	-2	2	29	0.0	-12	0.0
45	6.9	2	0	2	0	2	-31	0.0	13	0.0
46	13.6	0	0	2	0	0	26	0.0	-1	0.0
47	27.0	-1	0	2	0	1	21	0.0	-10	0.0
48	32.0	-1	0	0	2	1	16	0.0	-8	0.0
49	31.7	1	0	0	-2	1	-13	0.0	7	0.0
50	9.5	-1	0	2	2	1	-10	0.0	5	0.0
51	34.8	1	1	0	-2	0	-7	0.0	0	0.0
52	13.2	0	1	2	0	2	7	0.0	-3	0.0
53	14.2	0	-1	2	0	2	-7	0.0	3	0.0
54	5.6	1	0	2	2	2	-8	0.0	3	0.0
55	9.6	1	0	0	2	0	6	0.0	0	0.0
56	12.8	1	0	2	-2	2	6	0.0	-3	0.0
57	14.8	0	0	0	2	1	-6	0.0	3	0.0
58	7.1	0	0	2	2	1	-7	0.0	3	0.0
59	23.9	1	0	2	-2	1	6	0.0	-3	0.0
60	14.7	0	0	0	-2	1	-5	0.0	3	0.0
61	29.8	1	-1	0	0	0	5	0.0	0	0.0
62	6.9	2	0	2	0	1	-5	0.0	3	0.0
63	15.4	0	1	0	-2	0	-4	0.0	0	0.0
64	26.9	1	0	-2	0	0	4	0.0	0	0.0
65	29.5	0	0	0	1	0	-4	0.0	0	0.0
66	25.6	1	1	0	0	0	-3	0.0	0	0.0
67	9.1	1	0	2	0	0	3	0.0	0	0.0
68	9.4	1	-1	2	0	2	-3	0.0	1	0.0
69	9.8	-1	-1	2	2	2	-3	0.0	1	0.0
70	13.7	-2	0	0	0	1	-2	0.0	1	0.0
71	5.5	3	0	2	0	2	-3	0.0	1	0.0
72	7.2	0	-1	2	2	2	-3	0.0	1	0.0
73	8.9	1	1	2	0	2	2	0.0	-1	0.0
74	32.6	-1	0	2	-2	1	-2	0.0	1	0.0
75	13.8	2	0	0	0	1	2	0.0	-1	0.0
76	27.8	1	0	0	0	2	-2	0.0	1	0.0
77	9.2	3	0	0	0	0	1	0.0	0	0.0
78	9.3	0	0	2	1	2	2	0.0	-1	0.0
79	27.3	-1	0	0	0	2	1	0.0	-1	0.0
80	10.1	1	0	0	-4	0	-1	0.0	0	0.0

Table III cont.

1980 IAU Theory of Nutation

Index j	Period (days)	Argument coefficient k_{j1}	k_{j2}	k_{j3}	k_{j4}	k_{j5}	A_{0j} (0".0001)	A_{1j} (0".0001)	B_{0j} (0".0001)	B_{1j} (0".0001)
81	14.6	-2	0	2	2	2	1	0.0	-1	0.0
82	5.8	-1	0	2	4	2	-2	0.0	1	0.0
83	15.9	2	0	0	-4	0	-1	0.0	0	0.0
84	22.5	1	1	2	-2	2	1	0.0	-1	0.0
85	5.6	1	0	2	2	1	-1	0.0	1	0.0
86	7.3	-2	0	2	4	2	-1	0.0	1	0.0
87	9.1	-1	0	4	0	2	1	0.0	0	0.0
88	29.3	1	-1	0	-2	0	1	0.0	0	0.0
89	12.8	2	0	2	-2	1	1	0.0	-1	0.0
90	4.7	2	0	2	2	2	-1	0.0	0	0.0
91	9.6	1	0	0	2	1	-1	0.0	0	0.0
92	12.7	0	0	4	-2	2	1	0.0	0	0.0
93	8.7	3	0	2	-2	2	1	0.0	0	0.0
94	23.8	1	0	2	-2	0	-1	0.0	0	0.0
95	13.1	0	1	2	0	1	1	0.0	0	0.0
96	35.0	-1	-1	0	2	1	1	0.0	0	0.0
97	13.6	0	0	-2	0	1	-1	0.0	0	0.0
98	25.4	0	0	2	-1	2	-1	0.0	0	0.0
99	14.2	0	1	0	2	0	-1	0.0	0	0.0
100	9.5	1	0	-2	-2	0	-1	0.0	0	0.0
101	14.2	0	-1	2	0	1	-1	0.0	0	0.0
102	34.7	1	1	0	-2	1	-1	0.0	0	0.0
103	32.8	1	0	-2	2	0	-1	0.0	0	0.0
104	7.1	2	0	0	2	0	1	0.0	0	0.0
105	4.8	0	0	2	4	2	-1	0.0	0	0.0
106	27.3	0	1	0	1	0	1	0.0	0	0.0

Expressions similar to these are adopted for the free-core nutations:

$$\delta\psi = (A_{00} + A_{10}T)\sin(\omega_f T) + (A_{20} + A_{30}T)\cos(\omega_f T) \tag{2.91}$$

and

$$\delta\varepsilon = (B_{00} + B_{10}T)\cos(\omega_f T) + (B_{20} + B_{30}T)\sin(\omega_f T) \tag{2.92}$$

The nutation model thus contains a total of 856 parameters: A_{ij} (i=0,3; j=1,106) and B_{ij} (i=0,3; j=1,106) plus the free-nutation amplitudes A_{i0} (i=0,3), B_{i0} (i=0,3). The only nonzero *a priori* amplitudes are the A_{0j}, A_{1j}, B_{0j}, B_{1j} (j=1,106) given in Table III.

The nutation tweaks are just constant additive factors to the angles $\delta\psi$ and $\delta\varepsilon$:

$$\delta\psi \rightarrow \delta\psi + \Delta\psi \tag{2.93}$$

and

$$\delta\varepsilon \rightarrow \delta\varepsilon + \Delta\varepsilon \tag{2.94}$$

As a temporary measure to provide for a better nutation model than the one in Table III, which is known to be deficient at the milliarcsecond level, there is now a MASTERFIT option to employ the annual and semiannual amplitudes of Herring et al. (1986). In terms of the present notation, and in the units of Table III, these revised amplitudes are: $A_{0,9}$ = -13172.2, $B_{0,9}$ = 5732.8, $A_{0,10}$ = 1471.0, $B_{0,10}$ = 72.1 for the in-phase nutations, and $A_{2,9}$ = -8.3, $B_{2,9}$ = -2.9, $A_{2,10}$ = 15.8, $B_{2,10}$ = -2.2 for the out-of-phase terms. It is emphasised that, for the present, the default nutation model in MASTERFIT is just the 1980 IAU nutation model given in Table III.

2.8 PRECESSION

The next transformation in going from the terrestrial frame to the celestial frame is the rotation P. This is the precession transformation from mean equatorial coordinates of date to the equatorial coordinates of the reference epoch (*e.g.*, J2000). It is the transpose of the matrix given on page 7 of Melbourne et al. (1968):

$$P_{11} = \cos\zeta_A \cos\Theta_A \cos Z_A - \sin\zeta_A \sin Z_A \quad (2.95)$$

$$P_{12} = \cos\zeta_A \cos\Theta_A \sin Z_A + \sin\zeta_A \cos Z_A \quad (2.96)$$

$$P_{13} = \cos\zeta_A \sin\Theta_A \quad (2.97)$$

$$P_{21} = -\sin\zeta_A \cos\Theta_A \cos Z_A - \cos\zeta_A \sin Z_A \quad (2.98)$$

$$P_{22} = -\sin\zeta_A \cos\Theta_A \sin Z_A + \cos\zeta_A \cos Z_A \quad (2.99)$$

$$P_{23} = -\sin\zeta_A \sin\Theta_A \quad (2.100)$$

$$P_{31} = -\sin\Theta_A \cos Z_A \quad (2.101)$$

$$P_{32} = -\sin\Theta_A \sin Z_A \quad (2.102)$$

$$P_{33} = \cos\Theta_A \quad (2.103)$$

With the angular units in arc seconds, the arguments are:

$$\zeta_A = 2306.2181\,T + 0.30188\,T^2 + 0.017998\,T^3 \quad (2.104)$$

$$Z_A = 2306.2181\,T + 1.09468\,T^2 + 0.018203\,T^3 \quad (2.105)$$

$$\Theta_A = 2004.3109\,T - 0.42665\,T^2 - 0.041833\,T^3 \quad (2.106)$$

These expressions are given by Lieske et al. (1977) and by Kaplan (1981). This completes the standard model for the orientation of the Earth.

2.9 PERTURBATION ROTATION

This standard model for the rotation of the Earth as a whole may need a small incremental rotation about any one of the resulting axes. Define this perturbation rotation matrix as

$$\Omega = \Delta_x \Delta_y \Delta_z \quad (2.107)$$

where

$$\Delta_x = \begin{pmatrix} 1 & 0 & 0 \\ 0 & 1 & -\delta\Theta_x \\ 0 & \delta\Theta_x & 1 \end{pmatrix} \quad (2.108)$$

with $\delta\Theta_x$ being a small angle rotation about the x axis, in the sense of carrying y into z;

$$\Delta_y = \begin{pmatrix} 1 & 0 & \delta\Theta_y \\ 0 & 1 & 0 \\ -\delta\Theta_y & 0 & 1 \end{pmatrix} \quad (2.109)$$

with $\delta\Theta_y$ being a small angle rotation about the y axis, in the sense of carrying s into x; and

$$\Delta_z = \begin{pmatrix} 1 & -\delta\Theta_z & 0 \\ \delta\Theta_z & 1 & 0 \\ 0 & 0 & 1 \end{pmatrix} \tag{2.110}$$

with $\delta\Theta_z$ being a small angle rotation about the s axis, in the sense of carrying x into y. For angles of the order of 1 arc second we can neglect terms of order $\delta\Theta^2 R_E$ as they give effects on the order of 0.015 cm. Thus, in that approximation

$$\Omega = \begin{pmatrix} 1 & -\delta\Theta_z & \delta\Theta_y \\ \delta\Theta_z & 1 & -\delta\Theta_x \\ -\delta\Theta_y & \delta\Theta_x & 1 \end{pmatrix} \tag{2.111}$$

In general,

$$\delta\Theta_i = \delta\Theta_i(t) = \delta\Theta_{i0} + \delta\dot{\Theta}_i T + f_i(T) \tag{2.112}$$

which is the sum of an offset, a time-linear rate, and some higher order or oscillatory terms. Currently, only the offset and linear rate are implemented. In particular, a non-zero value of $\delta\dot{\Theta}_y$ is equivalent to a change in the precession constant. Setting

$$\delta\Theta_x = \delta\Theta_y = \delta\Theta_z = 0 \tag{2.113}$$

gives the effect of applying only the standard rotation matrices.

Starting with the Earth-fixed vector, $\mathbf{r}_0$, we have in sections 2.3 through 2.8 above shown how we obtain the same vector, $\mathbf{r}_c$, expressed in the celestial frame:

$$\mathbf{r}_c = \Omega PNUXY(\mathbf{r}_0 + \Delta) \tag{2.114}$$

2.10 EARTH ORBITAL MOTION

We now wish to transform these station locations from a geocentric celestial reference frame moving with the Earth to a celestial reference frame which is at rest relative to the center of mass of the Solar System. In this Solar System barycentric frame we will use these station locations to calculate the geometric delay (see Section 2.1 above). We will transform this time interval so obtained back to the frame in which the time delay is actually measured by the interferometer – the frame moving with the Earth.

Let Σ' be a geocentric frame moving with vector velocity = $\boldsymbol{\beta}c$ relative to a frame, Σ, at rest relative to the Solar System center of mass. Further, let $\mathbf{r}(t)$ be the position of a point (*e.g.*, station location) in space as a function of time, t, as measured in the Σ (Solar System barycentric) frame. In the Σ' (geocentric) frame, there is a corresponding position $\mathbf{r}'(t')$ as a function of time, t'. We normally observe and model $\mathbf{r}'(t')$ as shown in sections 2.3 through 2.8 above. However, in order to calculate the geometric delay in the Solar System barycentric frame (Σ), we will need the transformations of $\mathbf{r}(t)$ and $\mathbf{r}'(t')$, as well as of t and t', as we shift frames of reference. Measuring positions in units of light travel time, we have from Jackson (1975):

$$\mathbf{r}'(t') = \mathbf{r}(t) + (\gamma - 1)\mathbf{r}(t) \cdot \frac{\boldsymbol{\beta}\boldsymbol{\beta}}{\boldsymbol{\beta}^2} - \gamma\boldsymbol{\beta}t \tag{2.115}$$

$$t' = \gamma[t - \mathbf{r}(t) \cdot \boldsymbol{\beta}] \tag{2.116}$$

and for the inverse transformation:

$$\mathbf{r}(t) = \mathbf{r}'(t') + (\gamma - 1)\mathbf{r}'(t') \cdot \frac{\boldsymbol{\beta}\boldsymbol{\beta}}{\boldsymbol{\beta}^2} + \gamma\boldsymbol{\beta}t' \tag{2.117}$$

$$t = \gamma[t' + \mathbf{r}'(t') \cdot \boldsymbol{\beta}] \tag{2.118}$$

where

$$\gamma = (1 - \boldsymbol{\beta}^2)^{-1/2} \tag{2.119}$$

Let t_1 represent the time measured in the Solar System barycentric frame (Σ), at which a wave front crosses antenna 1 at position $\mathbf{r}_1(t_1)$. Let $\mathbf{r}_2(t_1)$ be the position of antenna 2 at this same time as measured in the Solar System barycentric frame. Also, let t_2^* be the time measured in this frame at which that same wave front intersects station 2. This occurs at the position $\mathbf{r}_2(t_2^*)$. Following section 2.1 above, we can calculate the geometric delay $t_2^* - t_1$. Transforming this time interval back to the Σ' (geocentric) frame, we obtain

$$t_2^{*\prime} - t_1' = \gamma(t_2^* - t_1) - \gamma[\mathbf{r}_2(t_2^*) - \mathbf{r}_1(t_1)] \cdot \boldsymbol{\beta} \tag{2.120}$$

Assume further that the motion of station #2 is rectilinear over this time interval. That assumption is not strictly true, but as discussed below it is sufficiently good such that the error made as a result of that assumption is much less than 1 cm in calculated delay. Thus,

$$\mathbf{r}_2(t_2^*) = \mathbf{r}_2(t_1) + \boldsymbol{\beta}_2(t_2^* - t_1) \tag{2.121}$$

which gives:

$$\mathbf{r}_2(t_2^*) - \mathbf{r}_1(t_1) = \mathbf{r}_2(t_1) - \mathbf{r}_1(t_1) + \boldsymbol{\beta}_2(t_2^* - t_1) \tag{2.122}$$

and

$$\begin{aligned} t_2^{*\prime} - t_1' &= \gamma(t_2^* - t_1) - \gamma[\mathbf{r}_2(t_1) - \mathbf{r}_1(t_1)] \cdot \boldsymbol{\beta} - \gamma\boldsymbol{\beta}_2 \cdot \boldsymbol{\beta}[t_2^* - t_1] \\ &= \gamma[(1 - \boldsymbol{\beta}_2 \cdot \boldsymbol{\beta})(t_2^* - t_1) - \gamma[\mathbf{r}_2(t_1) - \mathbf{r}_1(t_1)] \cdot \boldsymbol{\beta}] \end{aligned} \tag{2.123}$$

This is the expression for the geometric delay that would be observed in the geocentric (Σ') frame in terms of the geometric delay and station positions measured in the Solar System barycentric system (Σ).

Since our calculation starts with station locations given in the geocentric frame, it is convenient to obtain an expression for $[\mathbf{r}_2(t_1) - \mathbf{r}_1(t_1)]$ in terms of quantities expressed in the geocentric frame. To obtain such an expression consider two events $[\mathbf{r}_1'(t_1'),\ \mathbf{r}_2'(t_1')]$ that are geometrically separate, but simultaneous, in the geocentric frame, and occurring at time t_1'. These two events appear in the Solar System barycentric frame as:

$$\mathbf{r}_1(t_1) = \mathbf{r}_1'(t_1') + (\gamma - 1)\mathbf{r}_1'(t_1') \cdot \frac{\boldsymbol{\beta}\boldsymbol{\beta}}{\boldsymbol{\beta}^2} + \gamma\boldsymbol{\beta}t_1' \tag{2.124}$$

and as:

$$\mathbf{r}_2(t_2) = \mathbf{r}_2'(t_1') + (\gamma - 1)\mathbf{r}_2'(t_1') \cdot \frac{\boldsymbol{\beta}\boldsymbol{\beta}}{\boldsymbol{\beta}^2} + \gamma\boldsymbol{\beta}t_1' \tag{2.125}$$

where

$$t_2 - t_1 = \gamma[\mathbf{r}_2'(t_1') - \mathbf{r}_1'(t_1')] \cdot \boldsymbol{\beta} \tag{2.126}$$

With these three equations and the expression

$$\mathbf{r}_2(t_2) = \mathbf{r}_2(t_1) + \boldsymbol{\beta}_2[t_2 - t_1] \tag{2.127}$$

we may obtain the vector $\mathbf{r}_2(t_1)$:

$$\mathbf{r}_2(t_1) = \mathbf{r}_2'(t_1') + (\gamma - 1)\mathbf{r}_2'(t_1') \cdot \frac{\boldsymbol{\beta}\boldsymbol{\beta}}{\boldsymbol{\beta}^2} + \gamma\boldsymbol{\beta}t_1' - \gamma\boldsymbol{\beta}_2[\mathbf{r}_2'(t_1') - \mathbf{r}_1'(t_1')] \cdot \boldsymbol{\beta} \tag{2.128}$$

This is the position of station #2 at the time t_1 as observed in Σ. From this we obtain:

$$\mathbf{r}_2(t_1) - \mathbf{r}_1(t_1) = \mathbf{r}'_2(t'_1) - \mathbf{r}'_1(t'_1) + (\gamma - 1)[\mathbf{r}'_2(t'_1) - \mathbf{r}'_1(t'_1)] \cdot \frac{\boldsymbol{\beta}\boldsymbol{\beta}}{\beta^2} - \gamma\boldsymbol{\beta}_2[\mathbf{r}'_2(t'_1) - \mathbf{r}'_1(t'_1)] \cdot \boldsymbol{\beta} \tag{2.129}$$

As shown in section 2.1 above, all that is needed to obtain $t_2^* - t_1$ for the case of plane waves are the vectors $[\mathbf{r}_2(t_1) - \mathbf{r}_1(t_1)]$ and $\boldsymbol{\beta}_2$. For curved wave fronts we will need to know the individual station locations in the barycentric frame as well. These we obtain from (2.124) and (2.128) with t'_1 set equal to zero. Setting $t'_1 = 0$ is justified since the origin of time is arbitrary when we are trying to obtain time differences.

In the actual coding of these transformations, the relationship for the transformation of velocities is also needed. Taking differentials in (2.117) and (2.118) we have:

$$d\mathbf{r} = d\mathbf{r}' + (\gamma - 1)d\mathbf{r}' \cdot \frac{\boldsymbol{\beta}\boldsymbol{\beta}}{\beta^2} + \gamma\boldsymbol{\beta}dt' \tag{2.130}$$

$$dt = \gamma(dt' + d\mathbf{r}' \cdot \boldsymbol{\beta}) \tag{2.131}$$

Dividing to obtain $d\mathbf{r}/dt$ we obtain for station #2 in the Σ frame:

$$\boldsymbol{\beta}_2 = \frac{\boldsymbol{\beta}'_2 + (\gamma - 1)\boldsymbol{\beta}'_2 \cdot \frac{\boldsymbol{\beta}\boldsymbol{\beta}}{\beta^2} + \gamma\boldsymbol{\beta}}{\gamma(1 + \boldsymbol{\beta}'_2 \cdot \boldsymbol{\beta})} \tag{2.132}$$

For station #2 relative to the geocentric origin, we have from (2.62) and (2.63):

$$\boldsymbol{\beta}'_2 \approx \Omega PN \frac{dU}{dH} XY\mathbf{r}'_{2t}\omega_E \tag{2.133}$$

where

$$\omega_E = 7.2921151467 \times 10^{-5} \text{ rad/sec} \tag{2.134}$$

is the inertial rotation rate of the Earth as specified in Kaplan (1981), p.12. This is not a critical number since it is used only for station velocities, or to extrapolate Earth rotation forward for very small fractions of a day (*i.e.*, typically less than 1000 seconds). Actually, this expression is a better approximation than it might seem from the form since the errors in the approximation, $\frac{dH}{dt} = \omega_E$, are very nearly offset by the effect of ignoring the time dependence of PN.

The assumption of rectilinear motion can be shown to result in negligible errors. Using the plane wave front approximation (2.2), we can estimate the error $\delta\tau$ in the calculated delay if we have made an error $\Delta\boldsymbol{\beta}_2$ in our value for $\boldsymbol{\beta}_2$:

$$\delta\tau = \hat{\mathbf{k}} \cdot [\mathbf{r}_2(t_1) - \mathbf{r}_1(t_1)]\left[\frac{1}{1 - \hat{\mathbf{k}} \cdot (\boldsymbol{\beta}_2 + \Delta\boldsymbol{\beta}_2)} - \frac{1}{1 - \hat{\mathbf{k}} \cdot \boldsymbol{\beta}_2}\right] \approx \tau\Delta\boldsymbol{\beta}_2 \tag{2.135}$$

Further, from (2.132) above,

$$\Delta\boldsymbol{\beta}_2 \approx \Delta\boldsymbol{\beta}'_2 \tag{2.136}$$

since

$$\gamma \approx 1 + 10^{-8} \tag{2.137}$$

For the vector $\boldsymbol{\beta}'_2$ in a frame rotating with angular velocity ω, the error $\Delta\boldsymbol{\beta}'_2$ that accumulates in the time interval τ due to neglecting the rotation of that frame is

$$\Delta\boldsymbol{\beta}'_2 \approx \boldsymbol{\beta}_2\omega\tau \tag{2.138}$$

Thus for typical Earth-fixed baselines, where $\tau \leq 0.02$ sec, neglect of the curvilinear motion of station #2 due to the rotation of the Earth causes an error of $< 4 \times 10^{-14}$ sec, or 0.0012 cm, in the calculation of τ. Similarly, neglect of the orbital character of the Earth's motion causes an error of the order of 0.00024 cm maximum.

The position, $\mathbf{R}_E$, and velocity, $\boldsymbol{\beta}_E$, of the Earth's center about the center of mass of the Solar System are:

$$\mathbf{R}_E = -\frac{\sum m_i \mathbf{R}_i}{\sum m_i} \tag{2.139}$$

$$\boldsymbol{\beta}_E = -\frac{\sum m_i \boldsymbol{\beta}_i}{\sum m_i} \tag{2.140}$$

where the index i indicates the Sun, Moon, and all nine Solar System planets. m_i is the mass of the body indexed by i, while $\mathbf{R}_i$ and $\boldsymbol{\beta}_i$ are that body's center-of-mass position and velocity relative to the center of the Earth in the celestial frame. In a strict sense, the summation should be over all objects in the Solar System. Except for the Earth-Moon system, each planet mass represents not only that planet's mass, but also that of all its satellites. The $\mathbf{R}_i$ and $\boldsymbol{\beta}_i$ are obtained from the JPL planetary ephemeris (DE200 as of May, 1982) for the J2000.0 frame.

In this treatment we have neglected the general relativistic effects which arise from the fact that the Earth is spinning in a gravitational potential well. We also have neglected the fact that there are differences in the local Earth-caused gravitational potential between the two antenna locations. These deficiencies of the model have been estimated to cause errors of less than 0.6 cm in the measurement of a 6,000 km baseline (Thomas, 1975).

Working in a frame at rest with respect to the center of mass of the Solar System causes relativistic effects due to the motion of the Solar System in a "fixed frame" to be included in the mean position of the sources and in their proper motion. The effect of galactic rotation can be easily estimated. In the vicinity of the Sun, the period for galactic rotation is approximately 2.2×10^8 years. Our distance from the center is approximately 10 kpc $= 3.086 \times 10^{22}$ cm. Thus, our velocity is

$$\beta = \frac{v}{c} \approx \frac{2\pi R}{Tc} \approx 10^{-3} \tag{2.141}$$

For a source at zero galactic latitude, the maximum change in apparent position (over one half galactic rotation) is

$$\Delta\Theta \approx \frac{2\pi\beta}{\text{period}} \approx 6 \times 10^{-6} \text{arcsec/year} \tag{2.142}$$

Since a 1-arcsecond angle subtends a distance of 30 meters at one Earth radius, neglecting this effect is roughly equivalent to 0.015 cm/year on intercontinental baselines. It also is nearly one to two orders of magnitude smaller than the effects of typical source structure, though it is systematic.

2.11 ANTENNA GEOMETRY

The above work indicates how the time delay model would be calculated for two points fixed with respect to the Earth's crust. In practice, however, an antenna system does not behave as an Earth-fixed point. Not only are there instrumental delays in the system, but portions of the antenna move relative to the Earth. To the extent that instrumental delays are independent of the antenna orientation, they are indistinguishable to the interferometer from clock offsets and secular changes in these offsets. If necessary, these instrumental delays can be separated from clock properties by a careful calibration of each antenna system. That is a separate problem, treated as a calibration correction (*e.g.*, Thomas, 1981), and will not be addressed here.

However, the motions of the antennas relative to the Earth's surface must be considered since they are part of the geometric model. A fairly general antenna pointing system is shown schematically in figure 5. The unit vector, $\hat{\mathbf{s}}$, to the apparent source position is shown. Usually, a symmetry axis AD will point parallel to $\hat{\mathbf{s}}$. The point A on the figure also represents the end view of an axis which

allows rotation in the plane perpendicular to that axis. This axis is offset by some distance H from a second rotation axis BE. All points on this second rotation axis are fixed relative to the Earth. Consequently, any point along that axis is a candidate for the fiducial point which terminates this end of the baseline. The point we actually use is the point P. A plane containing axis A and perpendicular to BE intersects BE at the point P. This is somewhat an arbitrary choice, one of conceptual convenience.

Consider the plane Q which is perpendicular to the antenna symmetry axis, AD, and contains the antenna rotation axis A. For plane wave fronts this is an isophase plane (it coincides with the wave front). For curved wave fronts this deviates from an isophase surface by $\approx H^2/(2R)$, where R is the distance to the source, and H is taken as a typical antenna offset AP. For $H \approx 10$ meters, $R = R_{moon} = 60\ R_E \approx 3.6 \times 10^8$ meters, $H^2/(2R) \approx 1.4 \times 10^{-7}$ meters, and is totally negligible. R has to be 5 km, or $10^{-3} R_E$, before this deviation approaches 1 cm contribution. Consequently, for all anticipated applications of radio interferometry using high-gain radio antennas, the curvature of the wave front may be neglected in obtaining the effect on the time delay of the antenna orientation.

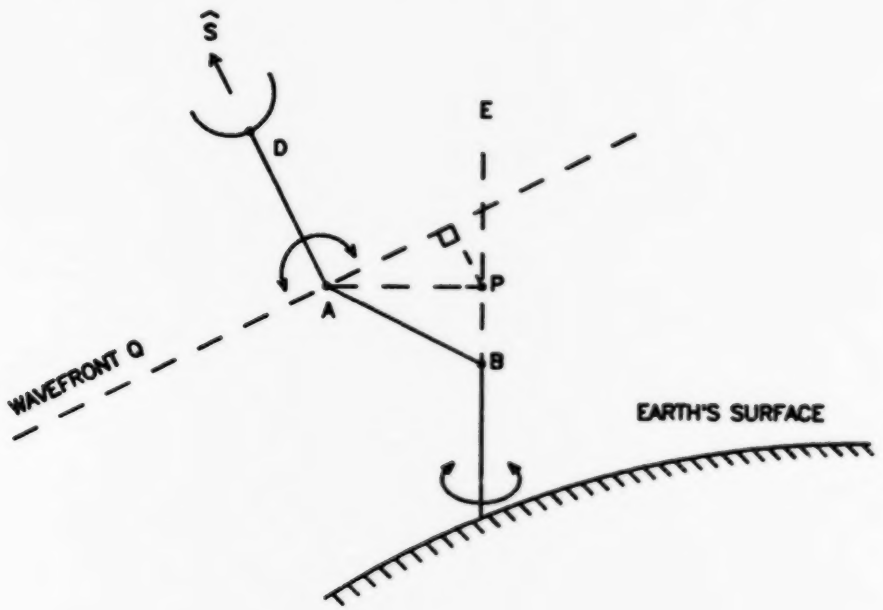

Figure 5. A generalized schematic representation of the geometry of a steerable antenna

Provided the instrumental delay of the antenna system is independent of the antenna orientation, the recorded signal is at a constant phase delay, independent of antenna orientation, at any point on the Q plane. Since this delay is indistinguishable from a clock offset, it will be totally absorbed by that portion of our model.

The advantage of choosing the Q plane rather than some other plane parallel to it is that the axis A is contained in this plane, and the axis A is fixed relative to the BE axis by the antenna structure. If l is the length of a line from P perpendicular to the Q plane, the wave front will reach the Earth-fixed

point P at a time $\Delta t = l/c$ after the wave front passes through the axis A. If τ_0 is the model delay for a wave front to pass from P on antenna #1 to a similarly defined point on antenna #2, then the model for the observed delay should be amended as:

$$\tau = \tau_0 - (\Delta t_2 - \Delta t_1) = \tau_0 + (l_1 - l_2)/c \tag{2.143}$$

where the subscripts refer to antennas #1 and #2.

For the inclusion of this effect in the model, we follow a treatment given by Wade (1970). Define a unit vector $\hat{\mathbf{I}}$ along BE, having a positive sense away from the Earth. Further, define a vector, $\mathbf{L}$, from P to A. Without much loss of generality in this antenna system, we assume that $\hat{\mathbf{s}}, \mathbf{L}$, and $\hat{\mathbf{I}}$ are coplanar. Then:

$$\mathbf{L} = \pm H \frac{\hat{\mathbf{I}} \times [\hat{\mathbf{s}} \times \hat{\mathbf{I}}]}{|\,\hat{\mathbf{I}} \times [\hat{\mathbf{s}} \times \hat{\mathbf{I}}]\,|} \tag{2.144}$$

where the plus or minus sign is chosen to give $\mathbf{L}$ the direction from P to A. The plus sign is used if, when $\hat{\mathbf{s}}$ and $\hat{\mathbf{L}}$ are parallel or antiparallel, the antenna comes closer to the source as H increases. Since

$$\hat{\mathbf{I}} \times [\hat{\mathbf{s}} \times \hat{\mathbf{I}}] = \hat{\mathbf{s}} - \hat{\mathbf{I}}\,[\hat{\mathbf{I}} \cdot \hat{\mathbf{s}}] \tag{2.145}$$

$$l = \hat{\mathbf{s}} \cdot \mathbf{L} = \pm H \sqrt{1 - [\hat{\mathbf{s}} \cdot \hat{\mathbf{I}}]^2} \tag{2.146}$$

where the sign choice above is carried through.

Curvature is always a negligible effect in the determination of $\hat{\mathbf{s}} \cdot \mathbf{L}$. Likewise, gravitational effects are sufficiently constant over a dimension $|\mathbf{L}|$ so as to be able to obtain to a very good approximation a single Cartesian frame over these dimensions. Consequently, it is somewhat easier to calculate a proper time $\Delta t = l/c$ in the antenna frame and to include it in the model by adding it to τ_0 , taking into account, in principle at least, the time dilation in going from the antenna frame to the frame in which τ_0 is obtained.

Thus, if $\hat{\mathbf{s}}_0$ is the unit vector to the source from the antenna in a frame at rest with respect to the Solar System center of mass, perform a Lorentz transformation to obtain $\hat{\mathbf{s}}$, the apparent source unit vector in the Earth-fixed celestial frame. Actually, the antenna does not "look" at the apparent source position $\hat{\mathbf{s}}$, but rather at the position of the source after the ray path has been refracted by an angle ε in the Earth's atmosphere. This effect is already included in the tropospheric delay correction (Section 4); however since the antenna model uses the antenna elevation angle E_0, the correction must be made here as well. For the worst case (elevation angle of 6°) at average DSN station altitudes, the deflection can be as large as 2×10^{-3} radians. Thus, $\delta l \approx H\varepsilon \approx 0.2$ cm for $H = 10$ meters. A model option permits modification of $\hat{\mathbf{s}}_0$ to take atmospheric refraction into account. The large-elevation-angle approximation is the inverse tangent law:

$$\Delta E = 3.13 \times 10^{-4} / \tan E_0 \tag{2.147}$$

where E is the elevation angle, and ΔE the change in apparent elevation induced by refraction. This model was implemented only for software comparison purposes, since it gives incorrect results at low elevation angles. In the notation of Section 4, a single homogeneous spherical layer approximation yields the bending correction

$$\Delta E = \cos^{-1}[\cos(E_0 + \alpha_0)/(1 + \chi_0)] - \alpha_0 \tag{2.148}$$

where

$$\chi_0 = (\rho z_{dry} + \rho z_{wet}/M_{001})/\Delta \tag{2.149}$$

$$\alpha_0 = \cos^{-1}[(1 + \sigma')/(1 + \sigma)] \tag{2.150}$$

$$\sigma = \Delta/R \tag{2.151}$$

$$\sigma' = \left[\left(1 + \sigma(\sigma + 2)/\sin^2 E_0\right)^{1/2} - 1\right] \sin^2 E_0 \tag{2.152}$$

This formula agrees with ray-tracing results to within 1% at 6° and ≈15% at 1° elevation, while the corresponding comparisons for Eq. (2.147) give ≈25% at 6° and a factor of 3 at 1°.

Since we are given $\hat{\mathbf{I}}$ in terrestrial coordinates, we first perform the coordinate transformation given by Q above:

$$\hat{\mathbf{I}} = Q\hat{\mathbf{I}}_{terrestrial} \tag{2.153}$$

With this done, obtain $\Delta t = l/c$, as shown in figure 6 for each of the major antenna types. Note that for "nearby" sources we also must include parallax (*e.g.*, geographically separate antennas are not pointing in the same direction). If $\mathbf{R}_0$ is the position of the source as seen from the center of the Earth, and $\mathbf{r}$ is the position of a station in the same frame, then the position of the source relative to that station is

$$\mathbf{R} = \mathbf{R}_0 - \mathbf{r} \tag{2.154}$$

and in (2.146) we make the substitution

$$[\hat{\mathbf{s}} \cdot \hat{\mathbf{I}}_j]^2 = \left[\frac{[\mathbf{R}_0 - \mathbf{r}] \cdot \hat{\mathbf{I}}}{|\mathbf{R}_0 - \mathbf{r}|}\right]^2 \tag{2.155}$$

$$l = \pm H\sqrt{1 - (\hat{S}\cdot\hat{I})^2}$$

AZ–EL		HOUR ANGLE – DEC	X–Y
INTERSECTING	OFFSET		
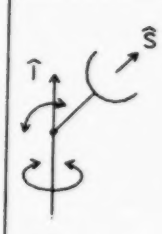	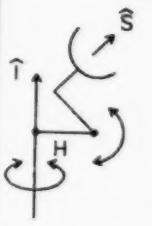	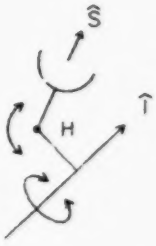	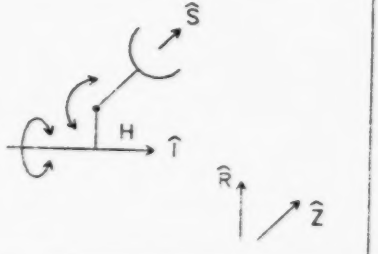
$H = 0$ $\Rightarrow l = 0$	$\hat{T}$ TOWARD GEODETIC VERTICAL $l = \pm H \cos$ (ELEVATION ANGLE)	$\hat{T}$ TOWARD NORTH POLE IN NORTHERN HEMISPHERE AND TOWARD SOUTH POLE IN SOUTHERN HEMISPHERE $l = \pm H \cos$ (SOURCE DECLINATION)	LET $\hat{Z}$ BE UNIT VECTOR TOWARD EARTH'S NORTH POLE $\hat{R}$ BE UNIT VECTOR TOWARD LOCAL GEODETIC VERTICAL THEN $\hat{T} = \dfrac{\hat{R} \times (\hat{Z} \times \hat{R})}{\lvert\hat{R} \times (\hat{Z} \times \hat{R})\rvert}$ AND $(\hat{S}\cdot\hat{I})^2 = \dfrac{[(\hat{S}\cdot\hat{Z})^2 - 2(\hat{S}\cdot\hat{Z})(\hat{S}\cdot\hat{R})(\hat{R}\cdot\hat{Z}) + (\hat{S}\cdot\hat{R})^2(\hat{R}\cdot\hat{Z})^2]}{1 - (\hat{R}\cdot\hat{Z})^2}$ $l = \pm H\sqrt{1 - (\hat{S}\cdot\hat{I})^2}$

Figure 6. Schematic representations of the four major antenna geometries used in VLBI

In the modeling software is the facility to provide a time-invariant offset vector in local geodetic coordinates (east, north, and local geodetic vertical) from this point (antenna location) to a point elsewhere, such as a benchmark on the ground. This is particularly useful in work involving transportable antennas which may be placed in slightly different places relative to an Earth-fixed benchmark each time a site is reoccupied. In modeling that offset vector, we make the assumption of a locally plane Earth-surface tangent to the geoid at the reference benchmark and the assumption that the local geodetic vertical for the antenna is parallel to that for the benchmark. With these assumptions there is an identity in the adjustments of antenna location with changes derived for the benchmark location. The error introduced by these assumptions in a baseline adjustment is approximately $\Delta B \times (d/R_E)$, where ΔB is the baseline adjustment from *a priori*, d is the separation of the antenna from the

benchmark, and R_E is the radius of the Earth. To keep this error smaller than 0.01 cm for baseline adjustments of the order of 1 meter, $d < 600$ meters is required.

More troublesome is that an error in obtaining the local vertical by an angle $\delta\Theta$, when using an antenna whose intersection of axes is a distance, H, above the ground, can cause an error of $H\sin\delta\Theta \approx H\delta\Theta$ in measuring the baseline to the benchmark (Allen, 1982). Unless this error is already absorbed into the actual measurement of the offset vector, care must be taken in setting up the antenna so as to make $\delta\Theta$ minimal. For a baseline error < 0.1 cm, and an antenna height of 10 meters, $\delta\Theta < 20$ arcseconds is required. Often plumb bobs are used to locate the antenna position relative to a mark on the ground. This mark is, in turn, surveyed to the benchmark. Even the difference in geodetic vertical from the vertical defined by the plumb bob may be as large as 1 arc minute, thus potentially causing an error of 0.3 cm for antennas of height 10 meters. Consequently, great care must be taken in these measurements, particularly if the site is to be repeatedly occupied by antennas of different sizes.

Another physical effect related to antenna structures is the differential feed rotation for circularly polarized receivers. Liewer (1985) has calculated the phase shift θ for various antenna types. It is zero for equatorially mounted antennas. For altazimuth mounts,

$$\tan\theta = \cos\phi\sin H/(\sin\phi\cos\delta - \cos\phi\sin\delta\cos H) \tag{2.156}$$

with ϕ = station latitude, H = hour angle, and δ = declination of the source. For X-Y mounts, two cases are distinguished: orientation $N - S$ or $E - W$. The respective rotation angles are

$$\tan(-\theta) = \sin\phi\sin H/(\cos\phi\cos\delta + \sin\phi\sin\delta\cos H) \qquad (N - S) \tag{2.157}$$

$$\tan(-\theta) = -\cos H/(\sin\delta\sin H) \qquad (E - W) \tag{2.158}$$

The effect cancels for group delay data, but can be significant for phase delay data. The effect on phase delay is

$$\tau = (\theta_2 - \theta_1)/f \tag{2.159}$$

where f is the observing frequency and θ_i the phase rotation at station i. The feed rotation correction is now an optional part of the MASTERFIT model.

2.12 PARTIAL DERIVATIVES OF DELAY WITH RESPECT TO GEOMETRIC MODEL PARAMETERS

With respect to any given parameter, the calculation of the time-delay model must be at least as accurate as the data is sensitive to that parameter. Consequently, such effects as the curvature of the wave fronts were considered. However, such detail is not necessary for determining the derivatives with respect to the relevant model parameters. Here, the plane wave approximation is sufficient. Iteration on the "solve-for" parameters and the rapid convergence of an expansion of the time delay in the relevant parameters about some *a priori* point permit this simplification.

In this plane wave approximation we wish to obtain the parameter derivatives with respect to:

1. the nominal baseline components (actually, station locations),
2. the parameters of the whole Earth orientation matrix Q described above,
3. the solid-Earth tidal parameters,
4. the parameters of source location (right ascension and declination),
5. the antenna axis offsets,
6. the constant, γ_{PPN}, in the retardation of the light ray due to gravitational effects.

The expressions for these derivatives are considerably simplified if tensor notation, with the Einstein summation convention, is employed. Before proceeding any further, we make the following definitions for this section:

τ = time delay modeled in the geocentric frame,
τ_s = this same time delay, but modeled in the Solar System center of mass frame,
$\hat{\mathbf{s}}$ = source unit vector (in the celestial system at rest with respect to the Solar System center of mass),
$\boldsymbol{\beta}$ = velocity of the geocentric frame as measured in the Solar System center of mass frame (remember, all distances are measured in time; thus, this quantity is dimensionless),
$\boldsymbol{\beta}_2$ = velocity of station #2 in Solar System center of mass frame,
$\rho = 1 + \hat{\mathbf{s}} \cdot \boldsymbol{\beta}_2$. This is a factor ≈ 1.0001, which arises from the motion of station #2 during the passage of the wave front from station #1 to #2,
$\gamma = (1 - \boldsymbol{\beta}^2)^{-1/2}$,
$\gamma_2 = (1 - \boldsymbol{\beta}_2^2)^{-1/2}$,
Q = matrix which transforms from the terrestrial system to the celestial system,
$\mathbf{L}_0$ = the baseline vector in the terrestrial system,
$\mathbf{L}_s$ = this same baseline vector in the celestial system center of mass frame,
$\mathbf{L}$ = this same baseline vector in the celestial system.

With these definitions (2.123) may be written

$$\tau = \gamma(1 - \boldsymbol{\beta} \cdot \boldsymbol{\beta}_2)\tau_s - \gamma \boldsymbol{\beta} \cdot \mathbf{L}_s \tag{2.160}$$

For plane waves from (2.2):

$$\tau_s = \frac{\hat{\mathbf{k}} \cdot [\mathbf{r}_2 - \mathbf{r}_1]}{1 - \hat{\mathbf{k}} \cdot \dot{\mathbf{r}}_2} = -\frac{\hat{\mathbf{s}} \cdot \mathbf{L}_s}{1 + \hat{\mathbf{s}} \cdot \boldsymbol{\beta}_2} = -\frac{\hat{\mathbf{s}} \cdot \mathbf{L}_s}{\rho} \tag{2.161}$$

Thus,

$$\tau = -\gamma[1 - \beta_{2_i}\beta_i]\frac{s_k L_{s_k}}{\rho} - \gamma \beta_k L_{s_k} \tag{2.162}$$

For parameters (represented symbolically by η) associated with L_{s_k} only:

$$\frac{\partial \tau}{\partial \eta} = -\left[\gamma(1 - \beta_{2_i}\beta_i)\frac{s_k}{\rho} + \gamma\beta_k\right]\frac{\partial L_{s_k}}{\partial \eta} \tag{2.163}$$

Define the vector:

$$\Psi_k = -\left[\gamma(1 - \beta_{2_i}\beta_i)\frac{s_k}{\rho} + \gamma\beta_k\right] \tag{2.164}$$

Then

$$\frac{\partial \tau}{\partial \eta} = \Psi_k \frac{\partial L_{s_k}}{\partial \eta} \tag{2.165}$$

For parameters associated with the source position only:

$$\frac{\partial \tau}{\partial \eta} = -\gamma(1 - \beta_2 \cdot \beta_i)\frac{L_{s_k}}{\rho}\left[\frac{\partial s_k}{\partial \eta} - \frac{s_k}{\rho}\frac{\partial \rho}{\partial \eta}\right] \tag{2.166}$$

Since

$$\rho = 1 + s_l \beta_{2_l} \tag{2.167}$$

$$\begin{aligned}\frac{\partial \tau}{\partial \eta} &= -\gamma(1 - \beta_2 \cdot \beta_i)\frac{L_{s_k}}{\rho}\left[\frac{\partial s_k}{\partial \eta} - \frac{s_k \beta_{2_l}}{\rho}\frac{\partial s_l}{\partial \eta}\right] \\ &= -\gamma(1 - \beta_2 \cdot \beta_i)\frac{L_{s_k}}{\rho}\left[\delta_{kl} - \frac{s_k \beta_{2_l}}{\rho}\right]\frac{\partial s_l}{\partial \eta}\end{aligned} \tag{2.168}$$

Define the vector:

$$M_j = -\gamma(1 - \beta_{2_l} \cdot \beta_l)\frac{L_{s_i}}{\rho}\left[\delta_{ij} - \frac{s_i \beta_{2_j}}{\rho}\right] \tag{2.169}$$

Then,

$$\frac{\partial \tau}{\partial \eta} = M_j \frac{\partial s_j}{\partial \eta} \tag{2.170}$$

For example:

$$\mathbf{s} = [\ \cos\delta\cos\alpha,\ \cos\delta\sin\alpha,\ \sin\delta\ ] \tag{2.171}$$

Then,

$$\frac{\partial s}{\partial \alpha} = [\ -\cos\delta\sin\alpha,\ \cos\delta\cos\alpha,\ 0\ ] = [\ A_1, A_2, A_3\ ] \tag{2.172}$$

and

$$\frac{\partial s}{\partial \delta} = [\ -\sin\delta\cos\alpha,\ -\sin\delta\sin\alpha,\ \cos\delta\ ] = [\ F_1, F_2, F_3\ ] \tag{2.173}$$

and

$$\frac{\partial \tau}{\partial \alpha} = M_i A_i \tag{2.174}$$

$$\frac{\partial \tau}{\partial \delta} = M_i F_i \tag{2.175}$$

Or, if we define the matrices:

$$G = \begin{pmatrix} A_1 & F_1 \\ A_2 & F_2 \\ A_3 & F_3 \end{pmatrix} \tag{2.176}$$

and

$$M = (\ M_1, M_2, M_3\ ) \tag{2.177}$$

then:

$$\left[\frac{\partial \tau}{\partial \alpha},\ \frac{\partial \tau}{\partial \delta}\right] = MG \tag{2.178}$$

For station location parameters the algebra is somewhat more complex. Since

$$\begin{aligned}\mathbf{L}_s &= \mathbf{r}_2(t_1) - \mathbf{r}_1(t_1) \\ &= \mathbf{r}_2(t_2) - \mathbf{r}_1(t_1) - \boldsymbol{\beta}_2[t_2 - t_1] \\ &= \mathbf{r}_2(t_2) - \mathbf{r}_1(t_1) - \gamma\boldsymbol{\beta}_2[\mathbf{r}_2'(t_1') - \mathbf{r}_1'(t_1')]\cdot\boldsymbol{\beta} \\ &= [\mathbf{r}_2'(t_1') - \mathbf{r}_1'(t_1')] + (\gamma - 1)[\mathbf{r}_2'(t_1') - \mathbf{r}_1'(t_1')]\cdot\hat{\boldsymbol{\beta}}\hat{\boldsymbol{\beta}} - \gamma\boldsymbol{\beta}_2\boldsymbol{\beta}\cdot[\mathbf{r}_2'(t_1') - \mathbf{r}_1'(t_1')]\end{aligned} \tag{2.179}$$

we have:

$$\mathbf{L}_s = \mathbf{L} + (\gamma - 1)\mathbf{L} \cdot \hat{\boldsymbol{\beta}}\hat{\boldsymbol{\beta}} - \gamma \boldsymbol{\beta}_2 \boldsymbol{\beta} \cdot \mathbf{L} \tag{2.180}$$

or in tensor notation

$$L_{s_i} = \left[\delta_{ij} + \left[\frac{(\gamma - 1)\beta_i}{\beta^2} - \gamma\beta_{2_i}\right]\beta_j\right] L_j \tag{2.181}$$

Define the tensor:

$$E_{ij} = \delta_{ij} + \left[\frac{(\gamma - 1)\beta_i}{\beta^2} - \gamma\beta_{2_i}\right]\beta_j \tag{2.182}$$

Then

$$L_{s_i} = E_{ij} L_j \tag{2.183}$$

Since

$$L_j = Q_{jk} L_{0_k} \tag{2.184}$$

$$L_{s_i} = E_{ij} Q_{jk} L_{0_k} \tag{2.185}$$

Thus,

$$\tau = \Psi_i E_{ij} Q_{jk} L_{0_k} \tag{2.186}$$

For parameters which are involved with station locations expressed in the terrestrial coordinate system:

$$\frac{\partial \tau}{\partial \eta} = [\Psi_i E_{ij} Q_{jk}] \frac{\partial L_{0_k}}{\partial \eta} = B_k \frac{\partial L_{0_k}}{\partial \eta} \tag{2.187}$$

where the vector element

$$B_k = \Psi_i E_{ij} Q_{jk} \tag{2.188}$$

Such parameters are: $r^0_{sp_i}$ (radius off spin axis), λ^0_i (longitude), z^0_i (height above the equator), $\dot{r}_{sp_i}$, $\dot{\lambda}_i$, $\dot{z}_i$ (their respective time rates), h_i (vertical Love number), l_i (horizontal Love number), ψ_i (phase lag of maximum tidal amplitude). The subscript refers to station number, *i.e.*, $i = 1, 2$. Define the matrix:

$$W = [-R_1, R_2, -\Lambda_1, \Lambda_2, -Z_1, Z_2, -\dot{R}_1, \dot{R}_2, -\dot{\Lambda}_1, \dot{\Lambda}_2, -\dot{Z}_1, \dot{Z}_2, -V_1, V_2, -H_1, H_2, -\Phi_1, \Phi_2] \tag{2.189}$$

where each column contains the partials of the L_0 component vectors x, y, z with respect to the parameters. For example, for the constant terms in the station coordinates [see Eqs. (2.37) through (2.39)]:

$$R_i = \begin{pmatrix} \dfrac{\partial L_{0_x}}{\partial r^0_{sp_i}} \\ \dfrac{\partial L_{0_y}}{\partial r^0_{sp_i}} \\ \dfrac{\partial L_{0_z}}{\partial r^0_{sp_i}} \end{pmatrix} = \begin{pmatrix} \cos\lambda^0_i \\ \sin\lambda^0_i \\ 0 \end{pmatrix} \tag{2.190}$$

$$\Lambda_i = \begin{pmatrix} \dfrac{\partial L_{0_x}}{\partial \lambda^0_i} \\ \dfrac{\partial L_{0_y}}{\partial \lambda^0_i} \\ \dfrac{\partial L_{0_z}}{\partial \lambda^0_i} \end{pmatrix} = \begin{pmatrix} -r^0_{sp_i} \sin\lambda^0_i \\ r^0_{sp_i} \cos\lambda^0_i \\ 0 \end{pmatrix} \tag{2.191}$$

$$Z_i = \begin{pmatrix} \frac{\partial L_{0_x}}{\partial z_i^0} \\ \frac{\partial L_{0_y}}{\partial z_i^0} \\ \frac{\partial L_{0_z}}{\partial z_i^0} \end{pmatrix} = \begin{pmatrix} 0 \\ 0 \\ 1 \end{pmatrix} \tag{2.192}$$

For the station coordinate rates,

$$\dot{R}_i = (t - t_0)R_i \qquad \dot{\Lambda}_i = (t - t_0)\Lambda_i \qquad \dot{Z}_i = (t - t_0)Z_i \tag{2.193}$$

From Eqs. (2.44) through (2.47), and relying on Williams (1970):

$$V_i = \begin{pmatrix} \frac{\partial \delta_{ix}}{\partial h_i} \\ \frac{\partial \delta_{iy}}{\partial h_i} \\ \frac{\partial \delta_{iz}}{\partial h_i} \end{pmatrix} = S(i)V(i)W(i) \begin{pmatrix} g_1(i) \\ 0 \\ 0 \end{pmatrix} \tag{2.194}$$

$$H_i = \begin{pmatrix} \frac{\partial \delta_{ix}}{\partial l_i} \\ \frac{\partial \delta_{iy}}{\partial l_i} \\ \frac{\partial \delta_{iz}}{\partial l_i} \end{pmatrix} = S(i)V(i)W(i) \begin{pmatrix} 0 \\ g_2(i) \\ g_3(i) \end{pmatrix} \tag{2.195}$$

$$\Phi_i = \begin{pmatrix} \frac{\partial \delta_{ix}}{\partial \psi_i} \\ \frac{\partial \delta_{iy}}{\partial \psi_i} \\ \frac{\partial \delta_{iz}}{\partial \psi_i} \end{pmatrix} = S(i)V(i)W(i) \begin{pmatrix} \frac{\partial g_1(i)}{\partial \psi_i} \\ \frac{\partial g_2(i)}{\partial \psi_i} \\ \frac{\partial g_3(i)}{\partial \psi_i} \end{pmatrix} \tag{2.196}$$

where $i = 1$ implies station #1, $i = 2$ implies #2, and $S(1) = -1$, while $S(2) = 1$. These partials of g with respect to ψ are

$$\frac{\partial g_{1_s}}{\partial \psi} = \frac{3\mu_s r_p^2}{R_s^5} h\mathbf{r}_p \cdot \mathbf{R}_s [X_s y_p - Y_s x_p] \tag{2.197}$$

$$\frac{\partial g_{2_s}}{\partial \psi} = \frac{3\mu_s r_p^2}{R_s^5} l \frac{|\mathbf{r}_p|}{\sqrt{x_p^2 + y_p^2}} \left[[\mathbf{r}_p \cdot \mathbf{R}_s][x_p X_s + y_p Y_s] - [Y_s x_p - X_s y_p]^2 \right] \tag{2.198}$$

$$\frac{\partial g_{3_s}}{\partial \psi} = \frac{3\mu_s r_p^2}{R_s^5} l [X_s y_p - Y_s x_p] \left[\sqrt{x_p^2 + y_p^2} Z_s - \frac{z_p}{\sqrt{x_p^2 + y_p^2}} [2\mathbf{r}_p \cdot \mathbf{R}_s - z_p Z_s] \right] \tag{2.199}$$

Also, define a vector:

$$D = \left[\frac{\partial \tau}{\partial r_{s_{p_1}}^0}, \frac{\partial \tau}{\partial r_{s_{p_2}}^0}, \frac{\partial \tau}{\partial \lambda_1^0}, \frac{\partial \tau}{\partial \lambda_2^0}, \frac{\partial \tau}{\partial z_1^0}, \frac{\partial \tau}{\partial z_2^0}, \frac{\partial \tau}{\partial \dot{r}_{s_{p_1}}}, \frac{\partial \tau}{\partial \dot{r}_{s_{p_2}}}, \frac{\partial \tau}{\partial \dot{\lambda}_1}, \frac{\partial \tau}{\partial \dot{\lambda}_2}, \frac{\partial \tau}{\partial \dot{z}_1}, \frac{\partial \tau}{\partial \dot{z}_2}, \right.$$
$$\left. \frac{\partial \tau}{\partial b_1}, \frac{\partial \tau}{\partial b_2}, \frac{\partial \tau}{\partial h_1}, \frac{\partial \tau}{\partial h_2}, \frac{\partial \tau}{\partial l_1}, \frac{\partial \tau}{\partial l_2}, \frac{\partial \tau}{\partial \psi_1}, \frac{\partial \tau}{\partial \psi_2} \right] \tag{2.200}$$

Then

$$D = BW \tag{2.201}$$

Certain parameters such as $UT1$, polar motion, precession, and nutation affect Q only. For these parameters

$$\frac{\partial \tau}{\partial \eta} = \Psi_i E_{ij} \left(\frac{\partial Q_{ik}}{\partial \eta} \right) L_{0_k} \tag{2.202}$$

Define a vector:

$$K_i = \Psi_k E_{ki} \tag{2.203}$$

Then

$$\frac{\partial \tau}{\partial \eta} = K_i \left(\frac{\partial Q_{ik}}{\partial \eta} \right) L_{0_k} \tag{2.204}$$

for parameters which affect only the orientation of the Earth as a whole.

A number of parameter partials are available for the orientation of the Earth. These are for $UT1$, X pole, Y pole, and nutation, as well as the angular offset and angular rate terms in the Earth orientation perturbation matrix Ω. From (2.62):

$$Q = \Omega PNUXY \tag{2.205}$$

Define the matrix:

$$Y' = \frac{\partial Y}{\partial \Theta_2} = \begin{pmatrix} 1 & 0 & 0 \\ 0 & -\sin\Theta_2 & \cos\Theta_2 \\ 0 & -\cos\Theta_2 & -\sin\Theta_2 \end{pmatrix} \tag{2.206}$$

Then, the partial required for the Y polar motion parameter is:

$$\frac{\partial Q}{\partial \Theta_y} = \Omega PNUXY' \tag{2.207}$$

An analogous technique is used for the X pole angle, and for $UT1$, working with the matrix partials $\frac{\partial X}{\partial \Theta_1}$, and $\frac{\partial U}{\partial (UT1)} = \frac{\partial U}{\partial H}$.

Partial derivatives of the VLBI obeervables with respect to the nutation amplitudes and tweaks appear formidable at first sight, but are relatively easy to evaluate if the calculation is performed in an organised fashion. Symbolising the parameters by η, we need to evaluate the partials of the matrix Q with respect to η:

$$\frac{\partial Q}{\partial \eta} = \Omega P \left(\frac{\partial N}{\partial \delta\psi} U + N \frac{\partial U}{\partial \delta\psi} \right) \frac{\partial \delta\psi}{\partial \eta} XY \tag{2.208}$$

$$\frac{\partial Q}{\partial \eta} = \Omega P \left(\frac{\partial N}{\partial \delta\varepsilon} U + N \frac{\partial U}{\partial \delta\varepsilon} \right) \frac{\partial \delta\varepsilon}{\partial \eta} XY \tag{2.209}$$

Since $\delta\varepsilon = \varepsilon - \bar{\varepsilon}$, the first partial on the rhs of Eq. (2.209) is equal to $\frac{\partial N}{\partial \varepsilon}$. The derivatives of N with respect to $\delta\psi$ and $\delta\varepsilon$ are easily obtained from the expression for N in Eq. (2.80):

$$\frac{\partial N}{\partial \delta\psi} = \begin{pmatrix} -\sin\delta\psi & \cos\varepsilon\cos\delta\psi & \sin\varepsilon\cos\delta\psi \\ -\cos\bar{\varepsilon}\cos\delta\psi & -\cos\bar{\varepsilon}\cos\varepsilon\sin\delta\psi & -\cos\bar{\varepsilon}\sin\varepsilon\sin\delta\psi \\ -\sin\bar{\varepsilon}\cos\delta\psi & -\sin\bar{\varepsilon}\cos\varepsilon\sin\delta\psi & -\sin\bar{\varepsilon}\sin\varepsilon\sin\delta\psi \end{pmatrix} \tag{2.210}$$

and

$$\frac{\partial N}{\partial \delta\varepsilon} = \begin{pmatrix} 0 & -\sin\varepsilon\sin\delta\psi & \cos\varepsilon\sin\delta\psi \\ 0 & -\cos\bar{\varepsilon}\sin\varepsilon\cos\delta\psi + \sin\bar{\varepsilon}\cos\varepsilon & \cos\bar{\varepsilon}\cos\varepsilon\cos\delta\psi + \sin\bar{\varepsilon}\sin\varepsilon \\ 0 & -\sin\bar{\varepsilon}\sin\varepsilon\cos\delta\psi - \cos\bar{\varepsilon}\cos\varepsilon & \sin\bar{\varepsilon}\cos\varepsilon\cos\delta\psi - \cos\bar{\varepsilon}\sin\varepsilon \end{pmatrix} \tag{2.211}$$

From Eq. (2.67), the partials of U with respect to η are

$$\frac{\partial U}{\partial \eta} = \begin{pmatrix} -\sin H & -\cos H & 0 \\ \cos H & -\sin H & 0 \\ 0 & 0 & 0 \end{pmatrix} \frac{\partial H}{\partial \eta} \tag{2.212}$$

and, from Eq. (2.72),

$$\frac{\partial H}{\partial \psi} = \cos\varepsilon/(\cos^2\delta\psi \;+\; \cos^2\varepsilon\sin^2\delta\psi) \tag{2.213}$$

$$\frac{\partial H}{\partial \delta\varepsilon} = -\sin\varepsilon\tan\delta\psi/(1 \;+\; \cos^2\varepsilon\tan^2\delta\psi) \tag{2.214}$$

give the required U-dependent terms in Eqs. (2.208) and (2.209).

Partials of $\delta\psi$ and $\delta\varepsilon$ with respect to the parameters A_{ij} and B_{ij} are obtained immediately from Eqs. (2.91) and (2.92). For the "free nutations",

$$\frac{\partial\delta\psi}{\partial A_{00}} = \sin\omega_f T, \qquad \frac{\partial\delta\varepsilon}{\partial B_{00}} = \cos\omega_f T \tag{2.215}$$

$$\frac{\partial\delta\psi}{\partial A_{10}} = T\sin\omega_f T, \qquad \frac{\partial\delta\varepsilon}{\partial B_{10}} = T\cos\omega_f T \tag{2.216}$$

$$\frac{\partial\delta\psi}{\partial A_{20}} = \cos\omega_f T, \qquad \frac{\partial\delta\varepsilon}{\partial B_{20}} = \sin\omega_f T \tag{2.217}$$

$$\frac{\partial\delta\psi}{\partial A_{30}} = T\cos\omega_f T, \qquad \frac{\partial\delta\varepsilon}{\partial B_{30}} = T\sin\omega_f T \tag{2.218}$$

and for the Wahr series terms ($j = 1$ to 106):

$$\frac{\partial\delta\psi}{\partial A_{0j}} = \sin\Big[\sum_{i=1}^{5} k_{ji}\alpha_i(T)\Big], \qquad \frac{\partial\delta\varepsilon}{\partial B_{0j}} = \cos\Big[\sum_{i=1}^{5} k_{ji}\alpha_i(T)\Big] \tag{2.219}$$

$$\frac{\partial\delta\psi}{\partial A_{1j}} = T\sin\Big[\sum_{i=1}^{5} k_{ji}\alpha_i(T)\Big], \qquad \frac{\partial\delta\varepsilon}{\partial B_{1j}} = T\cos\Big[\sum_{i=1}^{5} k_{ji}\alpha_i(T)\Big] \tag{2.220}$$

$$\frac{\partial\delta\psi}{\partial A_{2j}} = \cos\Big[\sum_{i=1}^{5} k_{ji}\alpha_i(T)\Big], \qquad \frac{\partial\delta\varepsilon}{\partial B_{2j}} = \sin\Big[\sum_{i=1}^{5} k_{ji}\alpha_i(T)\Big] \tag{2.221}$$

$$\frac{\partial\delta\psi}{\partial A_{3j}} = T\cos\Big[\sum_{i=1}^{5} k_{ji}\alpha_i(T)\Big], \qquad \frac{\partial\delta\varepsilon}{\partial B_{3j}} = T\sin\Big[\sum_{i=1}^{5} k_{ji}\alpha_i(T)\Big]. \tag{2.222}$$

Finally, the partials of the nutation matrix with respect to the "tweaks" $\Delta\psi$ and $\Delta\varepsilon$ are obtained by making the replacements (2.93) and (2.94) in N. $\dfrac{\partial N}{\partial\Delta\psi}$ and $\dfrac{\partial N}{\partial\Delta\varepsilon}$ are then seen to be identical to Eqs. (2.210) and (2.211) with the same replacements for $\delta\psi$ and $\delta\varepsilon$. If the *a priori* tweaks are zero, the partials are exactly equal to the expressions (2.210) and (2.211).

For the parameters in the perturbation matrix, Ω, from (2.112):

$$\frac{\partial\Omega}{\partial\delta\Theta_{x0}} = \begin{pmatrix} 0 & 0 & 0 \\ 0 & 0 & -1 \\ 0 & 1 & 0 \end{pmatrix} \tag{2.223}$$

$$\frac{\partial\Omega}{\partial\delta\dot{\Theta}_x} = \begin{pmatrix} 0 & 0 & 0 \\ 0 & 0 & -t \\ 0 & t & 0 \end{pmatrix} \tag{2.224}$$

where t is the number of years from the reference epoch (*e.g.*, J2000). Then, by substituting these matrices for Ω in (2.112), we obtain the appropriate partials of Q for perturbations about the x axis. By analogy, the perturbation parameters about the y and z axes may also readily be obtained.

If we seek the partials of parameters that affect only the "add-on" terms in $\tau = \tau_0 + \Delta\tau$, then from (2.123) we have:

$$\frac{\partial\tau}{\partial\eta} = \gamma(1 - \boldsymbol{\beta}\cdot\boldsymbol{\beta}_2)\frac{\partial(\Delta\tau)}{\partial\eta} \tag{2.225}$$

for terms which were "added on" in the Solar System barycenter. An example is gravitational bending:

$$\frac{\partial \tau}{\partial \gamma_{PPN}} = \gamma(1 - \boldsymbol{\beta} \cdot \boldsymbol{\beta}_2) \frac{\Delta_G}{(1 + \gamma_{PPN})} \tag{2.226}$$

For terms "added on" in the geocentric frame, then:

$$\frac{\partial \tau}{\partial \eta} = \frac{\partial \Delta \tau}{\partial \eta} \tag{2.227}$$

An example is the antenna offset vector. In this case:

$$\frac{\partial \tau}{\partial (\text{offset station } \#2)} = -\left[\pm\sqrt{1 - [\hat{\mathbf{s}} \cdot \hat{\mathbf{I}}]^2}\right] \tag{2.228}$$

and

$$\frac{\partial \tau}{\partial (\text{offset station } \#1)} = \pm\sqrt{1 - [\hat{\mathbf{s}} \cdot \hat{\mathbf{I}}]^2} \tag{2.229}$$

where the choice of sign for each station is determined by the choice of sign for that station in the model portion.

SECTION 3

CLOCK MODEL

The frequency standards ("clocks") at each of the two antennas are normally independent of each other. Attempts are made to synchronize them before an experiment by conventional synchronization techniques, but these techniques are accurate only to about 1 μsec in epoch and 10^{-12} in rate. More importantly, clocks often exhibit "jumps" and instabilities at a level that would greatly degrade interferometer accuracy. To account for these clock effects, an additional "delay" τ_c is included in the model delay, a delay that models the behavior of a station clock as a piecewise quadratic function of time throughout an observing session. Usually, however, we use only the linear portion of this model. For each station this clock model is given by:

$$\tau_c = \tau_{c1} + \tau_{c2}(t - t_{ref}) + \tau_{c3}(t - t_{ref})^2/2 \tag{3.1}$$

The term, t_{ref}, may be set by the user as a specific time (Julian date), or by default taken as the midpoint of the interval over which the *a priori* clock parameters, τ_{c1}, τ_{c2}, τ_{c3}, apply.

In addition to the effects of the lack of synchronization of clocks between stations, there are other differential instrumental effects which may contribute to the observed delay. In general, it is adequate to model these effects as if they were "clocklike". However, the instrumental effects on delays measured using the multifrequency bandwidth synthesis technique (Thomas, 1981) may be different from their effect on delays obtained from phase measurements at a single frequency.

The bandwidth synthesis process obtains delay from the slope of phase versus frequency $\left(\tau = \frac{\partial \phi}{\partial \nu}\right)$ across multiple frequency segments spanning the receiver passband. Thus, any instrumental contribution to the measured interferometer phase which is independent of frequency has no effect on the delay determined by the bandwidth synthesis technique. However, if delay is obtained directly from the phase measurement, ϕ, at a given frequency, ν, then this derived phase delay $\left(\tau_{pd} = \frac{\phi}{\nu}\right)$ does have that instrumental contribution.

Because of this difference, it is necessary to augment the "clock" model for phase delay measurements:

$$\tau_{c_{pd}} = \tau_c + \tau_{c4}(t - t_{ref}) + \tau_{c5}(t - t_{ref})^2/2 \tag{3.2}$$

where τ_c is the clock model for bandwidth synthesis observations and is defined in (3.1). Since the present system measures both bandwidth synthesis delay and phase delay rate, all of the clock parameters described above must be used. However, in a "perfectly" calibrated interferometer, $\tau_{c4} = \tau_{c5} = 0$. This particular model implementation allows simultaneous use of delay rate data derived from phase delay with delay data derived by means of the bandwidth synthesis technique. However, our particular software implementation currently is inconsistent with the simultaneous use of delay derived from bandwidth synthesis and delay obtained from phase delay measurements.

To model the interferometer delay on a given baseline, a difference of station clock terms is formed:

$$\tau_c = \tau_{c_{\text{station 2}}} - \tau_{c_{\text{station 1}}} \tag{3.3}$$

Specification of a reference clock is unnecessary until the parameter adjustment step, and need not concern us in the description of the model.

The partial derivatives of model delay with respect to the set of five parameters $(\tau_{c1}, \tau_{c2}, \tau_{c3}, \tau_{c4}, \tau_{c5})$ for each station are so trivial as to need no further explanation.

SECTION 4

TROPOSPHERE MODEL

In order to reach each antenna, the radio wave front must pass through the Earth's atmosphere. This atmosphere is made up of two components: the neutral atmosphere and the ionosphere. In turn, the neutral atmosphere is composed of two major constituents: the dry and the wet. The dry portion, primarily oxygen and nitrogen, is very nearly in hydrostatic equilibrium, and its effects can be accurately estimated simply by measuring the barometric pressure. Typically, at sea level in the local zenith direction, the additional delay that the incoming signal experiences due to the troposphere is approximately 2 meters. Except for winds aloft, unusually strong lee waves behind mountains (*e.g.*, Owens Valley, California), or very high pressure gradients, an azimuthally symmetric model based on measurements of surface barometric pressure is considered adequate. We have not yet investigated where this assumption breaks down, though "back-of-the-envelope" calculations indicate that, except in the unusual cases above, the error in such an assumption causes less than 1-cm error in the baseline.

Unfortunately, the wet component of the atmosphere (both water vapor and condensed water in the form of clouds) is not so easily modeled. The experimental evidence (Resch, 1983) is that it is "clumpy", and not azimuthally symmetric about the local vertical at a level which can cause many centimeters of error in a baseline measurement. Furthermore, because of incomplete mixing, surface measurements are very inadequate in estimating this contribution which even at zenith can reach 20 to 30 cm. Ideally, this tropospheric induced delay should be determined experimentally at each site. This is particularly true for short and intermediate (B < 1000 km) baselines, where the elevation angles of the two antennas are highly correlated in the observations. For long baselines, both the independence of the elevation angles at the two antennas, and the fact that often the mutual visibility requirements of VLBI constrain the antennas to look only in certain azimuthal sectors, allow the use of the interferometer data itself to estimate the effect of the water vapor as part of the parameter estimation process. For this reason, and because state-of-the-art water-vapor measurements are not always available, we also have the capability to model the neutral atmosphere at each station as a two-component effect, with each component being an azimuthally symmetric function of local geodetic elevation angle.

At each station the delay experienced by the incoming signal due to the troposphere can be modeled using a spherical-shell troposphere consisting of a wet component and a dry component:

$$\tau_{trop\ station\ i} = \tau_{wet\ trop} + \tau_{dry\ trop} \tag{4.1}$$

The total troposphere model for a given baseline is then:

$$\tau_t = \tau_{trop\ station\ 2} - \tau_{trop\ station\ 1} \tag{4.2}$$

If E is the apparent geodetic elevation angle of the observed source at station i, we have (dropping the subscript i):

$$\tau_{trop} = \rho_{Z_{dry}} R_{dry}(E) + \rho_{Z_{wet}} R_{wet}(E) \tag{4.3}$$

where ρ_Z is the additional delay at local zenith due to the presence of the troposphere, and R is an elevation angle mapping function.

For recent geodetic experiments, the observed delay has been corrected for the total tropospheric delay at each station, calculated on the basis of surface pressure measurements for the dry component, and water-vapor radiometer measurements for the wet component. This correction is recorded in the input data stream in such a way that it can be replaced by a new model. In the absence of such external calibrations, it was found that modeling the zenith delay as a linear function of time improves troposphere modeling considerably. The dry and wet zenith parameters are written as

$$\rho_{Z_{d,w}} = \rho^0_{Z_{d,w}} + \dot{\rho}_{Z_{d,w}}(t - t_0) \tag{4.4}$$

where t_0 is a reference time.

Since the model is linear in the parameters ρ^0 and $\dot{\rho}$, the partial derivatives with respect to zenith delays and rates are trivial. They are:

$$\frac{\partial \tau}{\partial \rho^0_{z_{i\,d\ or\ w}}} = f(i) R_{i\,d\ or\ w} \tag{4.5}$$

and

$$\frac{\partial \tau}{\partial \dot{\rho}_{z_{i\,d\ or\ w}}} = (t - t_0) f(i) R_{i\,d\ or\ w} \tag{4.6}$$

where $f(i) = 1$ for station #2, and -1 for station #1.

4.1 CHAO MAPPING FUNCTION

The simplest mapping function is that obtained by C. C. Chao (1974) through analytic fits to ray tracing, a function which he claims is accurate to the level of 1% at 6° elevation angle, and becomes much more accurate at higher elevation angles.

$$R_i = \frac{1}{\sin E + \dfrac{A_i}{\tan E + B_i}} \tag{4.7}$$

where

$$A_{dry} = 0.00143 \tag{4.8}$$

$$B_{dry} = 0.0445 \tag{4.9}$$

$$A_{wet} = 0.00035 \tag{4.10}$$

$$B_{wet} = 0.017 \tag{4.11}$$

The user must specify values for the zenith delays.

The partial derivatives of delay with respect to the parameters A_{dry} and B_{dry} are:

$$\frac{\partial \tau}{\partial A_{dry}} = -f(i) \rho_{z_{dry}} R^2_{dry} / (\tan E + B_{dry}) \tag{4.12}$$

and

$$\frac{\partial \tau}{\partial B_{dry}} = f(i) \rho_{z_{dry}} R^2_{dry} A_{dry} / (\tan E + B_{dry})^2 \tag{4.13}$$

where R_{dry} is the Chao mapping function, and E is the elevation angle.

4.2 LANYI MAPPING FUNCTION

Results of recent analyses of intercontinental data indicate that the Chao mapping function [Eq. (4.7)] is inadequate. To rectify this situation, two modifications have been made to the MASTERFIT code. First, the dry-troposphere mapping parameters A_{dry} and B_{dry} of the Chao mapping function R_{dry} have been promoted to the status of estimable parameters. Second, the code now permits the use of a new, more accurate analytic mapping function developed by Lanyi (1984). In its simplest form, this mapping function employs average values of atmospheric constants. Provision is made for specifying surface meteorological data acquired at the time of the VLBI experiments, which may override the average values. Using numerical fits to ray-tracing results, Davis et al. (1985) have arrived at another new mapping function, designated the CfA mapping function. Preliminary comparisons indicate that the Lanyi and CfA functions are in agreement to within the order of 1 to 2 cm over a wide range of atmospheric conditions down to 6° elevation angles. Finally, an approximate partial derivative is obtained with respect to one parameter in the Lanyi mapping function; this

permits adjustment even in the absence of surface data. The Lanyi function was made the default MASTERFIT troposphere model in early 1986.

Motivation for and full details of the development of a new tropospheric mapping function are given by Lanyi (1984). Here we attempt to give a minimal summary of the final formulas. The tropospheric delay is written as:

$$\tau_{trop} = F(E)/\sin E \tag{4.14}$$

where

$$F(E) = \rho_{Z_{dry}} F_{dry}(E) + \rho_{Z_{wet}} F_{wet}(E) + [\rho^2_{Z_{dry}} F_{b1}(E) + 2\rho_{Z_{dry}}\rho_{Z_{wet}} F_{b2}(E) + \rho^2_{Z_{wet}} F_{b3}(E)]/\Delta + \rho^3_{Z_{dry}} F_{b4}(E)/\Delta^2 \tag{4.15}$$

The quantities $\rho_{Z_{dry}}$ and $\rho_{Z_{wet}}$ have the usual meaning: zenith dry and wet tropospheric delays. Δ is the atmospheric scale height, $\Delta = kT_0/mg_c$, with k = Boltzmann's constant, T_0 = average surface temperature, m = mean molecular mass of dry air, and g_c = gravitational acceleration at the center of gravity of the air column. With the standard values $k = 1.38066 \times 10^{-16}$ erg/K, $m = 4.8097 \times 10^{-23}$ g, $g_c = 978.37$ erg/g·cm, and the average temperature for DSN stations $T_0 = 292$ K, the scale height $\Delta = 8567$ m.

The dry, wet, and bending contributions to the delay, $F_{dry}(E)$, $F_{wet}(E)$, and $F_{b1,b2,b3,b4}(E)$, are expressed in terms of moments of the refractivity as

$$F_{dry}(E) = A_{10}(E)G(\lambda M_{110}, u) + 3\sigma u M_{210} G^3(M_{110}, u)/4 \tag{4.16}$$

$$F_{wet}(E) = A_{01}(E)G(\lambda M_{101}/M_{001}, u)/M_{001} \tag{4.17}$$

$$F_{b1}(E) = [\sigma G^3(M_{110}, u)/\sin^2 E - M_{020} G^3(M_{120}/M_{020}, u)]/2\tan^2 E \tag{4.18}$$

$$F_{b2}(E) = -M_{011} G^3(M_{111}/M_{011}, u)/2M_{001}\tan^2 E \tag{4.19}$$

$$F_{b3}(E) = -M_{002} G^3(M_{102}/M_{002}, u)/2M^2_{001}\tan^2 E \tag{4.20}$$

$$F_{b4}(E) = M_{030} G^3(M_{130}/M_{030}, u)/2\tan^4 E \tag{4.21}$$

A misprinted sign in the last of Eqs. (5) of Appendix B of Lanyi (1984) has been corrected in Eq. (4.21). Here $G(q,u)$ is a geometric factor given by

$$G(q, u) = (1 + qu)^{-1/2} \tag{4.22}$$

with

$$u = 2\sigma/\tan^2 E \tag{4.23}$$

where σ is a measure of the curvature of the Earth's surface Δ/R with standard value 0.001345.

The quantities $A_{lm}(E)$ and M_{ilm} are related to moments of the atmospheric refractivity, and are defined below. $A_{10}(E)$ involves the dry refractivity, while $A_{01}(E)$ is the corresponding wet quantity. The $A_{lm}(E)$ are given by

$$A_{lm}(E) = M_{0lm} + \sum_{n=1}^{10}\sum_{k=0}^{n} \frac{(-1)^{n+k}(2n-1)!!M_{n-k,l,m}}{2^n k!(n-k)!}\left[\frac{u}{1+\lambda u M_{1lm}/M_{0lm}}\right]^n \left[\frac{\lambda M_{1lm}}{M_{0lm}}\right]^k \tag{4.24}$$

with the scale factor $\lambda = 3$ for $E < 10°$ and $\lambda = 1$ for $E > 10°$. Only the two combinations $(l, m) =$ (0,1) and (1,0) are needed for the $A_{lm}(E)$. The moments of the dry and wet refractivities are defined as

$$M_{nij} = \int_0^\infty dq\; q^n f^i_{dry}(q) f^j_{wet}(q) \tag{4.25}$$

where $f_{dry,\ wet}(q)$ are the surface-normalized refractivities. Here, n ranges from 0 to 1, i from 0 to 3, and j from 0 to 2; not all combinations are needed. Carrying out the integration in Eq. (4.25) for a three-section temperature profile gives an expression for the general moment M_{nij}:

$$M_{nij}/n! = (1 - e^{-aq_1})/a^{n+1} + e^{-aq_1}\left[1 - T_2^{b+n+1}(q_1, q_2)\right]\prod_{i=0}^{n}\frac{a}{b+i+1} + e^{-aq_1}T_2^{b+n+1}(q_1, q_2)/a^{n+1} \tag{4.26}$$

Here,

$$T_2(q_1, q_2) = 1 - (q_2 - q_1)/\alpha \tag{4.27}$$

The quantities q_1 and q_2 are the scale-height normalized inversion and tropopause altitudes, respectively. For the standard atmospheric model, $q_1 = 0.1459$ and $q_2 = 1.424$. The constants a and b are functions of the dry ($\alpha = 5.0$) and wet ($\beta = 3.5$) model parameters, as well as of the powers of the refractivities (i and j) in the moment definitions. Table IV gives the necessary a's and b's.

Table IV

Dependence of the Constants a and b on Tropospheric Model Parameters

i	j	a	b
1	0	1	α-1
0	1	β	$\alpha\beta - 2$
2	0	2	$2(\alpha - 1)$
1	1	$\beta + 1$	$\beta(\alpha + 1) - 3$
0	2	2β	$2(\alpha\beta - 2)$
3	0	3	$3(\alpha - 1)$

Note that the normalization is such that $M_{010} = 1$; this moment has therefore not been explicitly written in Eqs. (4.16) through (4.21).

At present, provision is made for input of four meteorological parameters to override the standard (average) values of the Lanyi model. These are: 1) the surface temperature T_0, which determines the atmosphere scale height (default value 292 K); 2) the temperature lapse rate W, which determines the dry model parameter α (default values $W = 6.8165$ K/km, $\alpha = 5.0$); 3) the inversion altitude h_1, which determines $q_1 = h_1/\Delta$ (default value $h_1 = 1.25$ km); and 4) the tropopause altitude h_2, which determines $q_2 = h_2/\Delta$ (default value $h_2 = 12.2$ km). A fifth parameter, the surface pressure p_0, is not used at present. Approximate sensitivity of the tropospheric delay (at 6° elevation) to the meteorological parameters is -0.7 cm/K for surface temperature, 2 cm/(K/km) for lapse rate, and -2 cm/km for inversion and 0.5 cm/km for tropopause altitude, respectively.

Partials of the delay with respect to the dry and wet zenith delays are obtained from Eqs. (4.14) and (4.15):

$$\frac{\partial \tau}{\partial \rho z_{dry}} = f(i)\left[F_{dry}(E) + 2\rho z_{dry} F_{b1}(E)/\Delta\right]/\sin E + \left[2\rho z_{wet} F_{b2}(E)/\Delta + 3\rho^2_{z_{dry}} F_{b4}(E)/\Delta^2\right]/\sin E \tag{4.28}$$

$$\frac{\partial \tau}{\partial \rho z_{wet}} = f(i)\left[F_{wet}(E) + 2\rho z_{dry} F_{b2}(E)/\Delta + 2\rho z_{wet} F_{b3}(E)/\Delta\right]/\sin E \tag{4.29}$$

In analysis of data for which meteorological parameters are not available, it is convenient to introduce an approximation to the mapping function [Eqs. (4.14) and (4.15)] which involves a one-parameter estimate. This parameter p accounts for deviations from standard meteorological conditions. The tropospheric delay is expressed as

$$\tau = (\rho z_{dry} + \rho z_{wet})/\sin E + p\frac{\partial \tau}{\partial p} \tag{4.30}$$

where the partial derivative is

$$\frac{\partial \tau}{\partial p} = -\frac{(\rho z_{dry} + \rho z_{wet}) u M_{110}}{G(M_{110}, u)\left[1 + G(M_{110}, u)\right] \sin E} + \frac{\rho z_{wet} u (M_{110} - M_{101}/M_{001})}{G(M_{110}, u) G(M_{101}/M_{001}, u)\left[G(M_{110}, u) + G(M_{101}/M_{001}, u)\right] \sin E} \tag{4.31}$$

4.3 CFA MAPPING FUNCTION

Another approach to improved modeling of tropospheric delay was recently published by Davis et al. (1985). Analytic fits to ray-tracing results yield the CfA mapping function

$$R_i = \frac{1}{\sin E + \dfrac{a}{\tan E + \dfrac{b}{\sin E + c}}} \tag{4.32}$$

where E is the elevation angle. The three parameters a, b, c are expressed in terms of meteorological data as

$$a = 0.0002723\,[\,1 + 2.642 \times 10^{-4} p_0 - 6.400 \times 10^{-4} e_0 + 1.337 \times 10^{-2} T_0 - 8.550 \times 10^{-2} \alpha - 2.456 \times 10^{-2} h_2\,] \tag{4.33}$$

$$b = 0.0004703\,[\,1 + 2.832 \times 10^{-5} p_0 + 6.799 \times 10^{-4} e_0 + 7.563 \times 10^{-3} T_0 - 7.390 \times 10^{-2} \alpha - 2.961 \times 10^{-2} h_2\,] \tag{4.34}$$

$$c = -0.0090 \tag{4.35}$$

Here, p_0 is the surface pressure and e_0 the surface partial water vapor pressure, both measured in millibars. The quantities T_0, α, and h_2 have the same meaning and units as in Section 4.2. This function is one of three optional mapping functions in the MASTERFIT model. In connection with testing parameter estimation for the Lanyi function, the partial derivative of delay with respect to surface temperature T_0 in the CfA function was also evaluated. It is

$$\frac{\partial \tau}{\partial T_0} = -\frac{\rho z_{dry} R_{dry}^2 \left[3.641 \times 10^{-6} (\sin E + c)[\tan E + b/(\sin E + c)] - 3.557 \times 10^{-6} a\right]}{(\sin E + c)[\tan E + b/(\sin E + c)]^2} \tag{4.36}$$

SECTION 5

IONOSPHERE MODEL

The second component of the Earth's atmosphere, the ionosphere, is a layer of plasma at about 350 km altitude, created primarily by the ultraviolet portion of the sunlight. In the quasi-longitudinal approximation (Spitzer, 1967) the refractive index of this medium is

$$n = \left[1 - \left(\frac{\nu_p}{\nu}\right)^2 \left(1 \pm \frac{\nu_g}{\nu}\cos\Theta\right)^{-1}\right]^{1/2} \tag{5.1}$$

where the plasma frequency, ν_p, is

$$\nu_p = \left(\rho c^2 r_0/\pi\right)^{1/2} \approx 8.97 \times 10^3 \rho^{1/2} \tag{5.2}$$

the electron gyrofrequency, ν_g, is

$$\nu_g = \frac{eB}{2\pi mc} \tag{5.3}$$

and Θ is the angle between the magnetic field B and the direction of propagation of the wave front. Here ρ is the number density of the electrons, and r_0 is the classical electron radius.

For the Earth's ionosphere, with $\rho \approx 10^{12}$ electrons m^{-3}, $\nu_p \approx 8.9$ MHz, while for the interplanetary medium with $\rho \approx 10^7 - 10^8$ electrons m^{-3}, $\nu_p \approx 28 - 89$ kHz. In the interstellar medium, $\rho \approx 10^5$ electrons m^{-3}, which gives $\nu_p \approx 3$ kHz. At typical microwave frequencies used for geodetic VLBI (8.4 GHz), $\nu_p/\nu = 10^{-3}$ for the ionosphere, 10^{-5} for the interplanetary medium, and 3×10^{-7} for the interstellar medium.

The gyrofrequency, ν_g, for an electron in the ≈ 0.2 gauss field of the Earth is ≈ 0.6 MHz. Thus, for the ionosphere, $\nu_g/\nu \approx 2 \times 10^{-4}$ at S band (2.3 GHz), and $\nu_g/\nu \approx 7 \times 10^{-5}$ at X band (8.4 GHz). For the interstellar medium $B \approx 10^{-6}$ gauss, while for the interplanetary region $B \approx 10^{-4}$ gauss.

Relative to vacuum as a reference, the phase delay of a monochromatic signal transiting this medium of refractive index, n, is

$$\tau_{pd} = \frac{1}{c}\int (n-1)dl \approx -\frac{1}{2c}\int \left(\frac{\nu_p'}{\nu}\right)^2 \left[1 + \frac{1}{4}\left(\frac{\nu_p'}{\nu}\right)^2 + \frac{1}{8}\left(\frac{\nu_p'}{\nu}\right)^3 + \ldots\right] dl \tag{5.4}$$

where

$$\frac{\nu_p'}{\nu} = \left(\frac{\nu_p}{\nu}\right)\left[1 \pm \left(\frac{\nu_g}{\nu}\right)\cos\Theta\right]^{-1/2} \tag{5.5}$$

For 8.4 GHz, we may approximate this effect to parts in $10^6 - 10^7$ by:

$$\Delta_{pd} \approx \frac{-q}{\nu^2}\left[1 \pm \overline{\left(\frac{\nu_g}{\nu}\right)\cos\Theta}\right]^{-1} \approx \frac{-q}{\nu^2}\left[1 - \overline{\left(\frac{\pm\nu_g}{\nu}\right)\cos\Theta}\right] \tag{5.6}$$

where

$$q = \frac{cr_0}{2\pi}\int \rho dl = \frac{cr_0 I_e}{2\pi} \tag{5.7}$$

and where I_e is the total number of electrons per unit area along the integrated line of sight. If we also neglect the term $\overline{(\nu_g \cos\Theta)}/\nu$, then the expression for Δ_{pd} becomes simple and independent of the geometry of the traversal of the wave front through the ionosphere:

$$\Delta_{pd} = -q/\nu^2 \tag{5.8}$$

This delay is negative. Thus, a phase advance actually occurs for a monochromatic signal. Since phase delay is obtained at a single frequency, delays derived from phase delay (*e.g.*, delay rates) experience

a delay increment which is negative (the actual delay with the medium present is less than what would be measured without the medium). In constrast, delays measured by means of a group delay technique such as bandwidth synthesis $\left(\tau = \frac{\partial \phi}{\partial \nu}\right)$ experience an additive delay which can be derived from (5.8) by differentiating $\phi = \nu \Delta_{pd}$ with respect to frequency.

$$\Delta_{gd} = q/\nu^2 \tag{5.9}$$

Notice that the sign is now positive, though the group delay is of the same magnitude as the phase delay advance. For group delay measurements, the measured delay is larger with the medium present than without the medium.

For a typical ionosphere, $\tau \approx 1 - 20 \times 10^{-10}$ sec at local zenith for $\nu = 8.4$ GHz. This effect has a maximum at approximately 1400 hours local time and a broad minimum during local night. For long baselines, the effects at each station are quite different. Thus, the differential effect may be of the same order as the maximum.

For the interplanetary medium and at an observing frequency of 8.4 GHz, a single ray path experiences a delay of approximately 6×10^{-7} sec in transiting the Solar System. However, the differential between the ray paths to the two stations on the Earth is considerably less, since the gradient between the two ray paths should also be inversely proportional to the dimensions of the plasma region (*e.g.*, one astronomical unit as opposed to a few thousand kilometers). The ray path from a source at a distance of 1 megaparsec (3×10^7 km) experiences an integrated plasma delay of approximately 5000 seconds for a frequency of 8.4 GHz. In this case, however, the typical dimension is also that much greater, and so the differential effect on two ray paths separated by one Earth radius is still not as great as the differential delays caused by the Earth's ionosphere.

These plasma effects can best be removed by the technique of observing the sources at two frequencies, ν_1 and ν_2, where $\nu_{1,2} \gg \nu_p$ and where $|\nu_2 - \nu_1|/(\nu_2 + \nu_1) \approx 1$. Then at the two frequencies ν_1 and ν_2 we obtain

$$\tau_{\nu 1} = \tau + q/\nu_1^2 \tag{5.10}$$

and

$$\tau_{\nu 2} = \tau + q/\nu_2^2 \tag{5.11}$$

Multiplying each expression by the square of the frequency involved and subtracting, we obtain

$$\tau = a\tau_{\nu 2} + b\tau_{\nu 1} \tag{5.12}$$

where

$$a = \frac{\nu_2^2}{\nu_2^2 - \nu_1^2} \tag{5.13}$$

and

$$b = \frac{-\nu_1^2}{\nu_2^2 - \nu_1^2} \tag{5.14}$$

This linear combination of the observables at two frequencies thus removes the charged particle contribution to the delay.

For uncorrelated errors in the frequency windows, the overall error in the derived delay can be modeled as

$$\sigma_\tau^2 = a^2 \sigma_{\tau_{\nu 2}}^2 + b^2 \sigma_{\tau_{\nu 1}}^2 \tag{5.15}$$

Modeling of other error types is more difficult and will not be treated in this report. Since the values of a and b are independent of q, these same coefficients apply both to group delay and to phase delay.

If we had not neglected the effect of the electron gyrofrequency in the ionosphere, then instead of (5.12) above, we would have obtained

$$\tau = a\tau_{\nu 2} + b\tau_{\nu 1} + \frac{q\,\overline{\nu_g \cos\Theta}}{\nu_2 \nu_1 (\nu_2 - \nu_1)} \tag{5.16}$$

where a and b are defined as in (5.13) and (5.14), respectively.

If we express the third term on the right-hand side in units of the contribution of the ionosphere at frequency ν_2, we obtain

$$\tau = a\tau_{\nu 2} + b\tau_{\nu 1} + \frac{\Delta_{pd}\nu_2 \overline{\nu_g \cos\Theta}}{\nu_1(\nu_2 + \nu_1)} \tag{5.17}$$

For X band $\Delta_{pd} \approx 1 - 20 \times 10^{-10}$ sec at the zenith. When using S band as the other frequency in the pair, this third term is $\approx 2 \times 10^{-4}\Delta_{pd}\cos\Theta \approx 2 - 40 \times 10^{-13}$ sec at zenith. In the worst case of high ionospheric electron content, and at low elevation angles, this effect could reach 0.1 cm of total error in determining the total delay using the simple formula (5.12) above. Notice that the effect becomes much more significant at lower frequencies.

In the software chain used at JPL, the dual-frequency correction is performed prior to the processing step "MASTERFIT". MASTERFIT does not have the facility to perform this correction. However, the process is described here because it is important to understanding the data input to MASTERFIT. For millimeter accuracy, or for lower observing frequencies even at centimeter accuracy levels, a correction for the gyrofrequency effect is necessary.

In the absence of the dual-frequency observation capability described above, one can improve the model of the interferometer by modeling the ionosphere, using whatever measurements of the total electron content are available. The model we have chosen to implement is very simple. Its formalism is very similar to that of the troposphere model, except that the ionosphere is modeled as a spherical shell for which the bottom is at the height h_1, above the geodetic surface of the Earth, and the top of the shell is at the height h_2, above that same surface (see figure 7). For each station the ionospheric delay is modeled as

$$\tau_i = kgI_eS(E)/\nu^2 \tag{5.18}$$

where

$$k = \frac{0.1c\tau_0}{2\pi} \tag{5.19}$$

I_e is the total electron content at zenith (in electrons per meter squared $\times 10^{-17}$), and $g = 1(-1)$ for group (phase) delay. E is the apparent geodetic elevation angle of the source, $S(E)$ is a slant range factor discussed below, and ν is the observing frequency in gigaherts.

The slant range factor (see figure 7) is

$$S(E) = \frac{\sqrt{R^2\sin^2 E + 2Rh_2 + h_2^2} - \sqrt{R^2\sin^2 E + 2Rh_1 + h_1^2}}{h_2 - h_1} \tag{5.20}$$

This expression is strictly correct for a spherical Earth of radius R, and a source at apparent elevation angle E. The model employed uses this expression and a geoid surface with a local radius of curvature at the receiving station of R equal to the distance from the receiving station to the center of the Earth. The model also assumes this same value of R can be used at the ionospheric penetration points, *e.g.*:

$$R_i = R + h_i \tag{5.21}$$

This is not strictly true, but is a very close approximation, particularly compared to the crude nature of the total electron content determinations on which the model also depends. The total ionospheric contribution on a given baseline is

$$\tau_I = \tau_{i_{\text{station 2}}} - \tau_{i_{\text{station 1}}} \tag{5.22}$$

We assume that the ionospheric total electron content, I_e, is the sum of two parts, one obtained by some external set of measurements such as Faraday rotation, and the other by some specified additive constant:

$$I_e = I_{e\ meas} + I_{e\ add} \tag{5.23}$$

These external measurements, in general, are not along directions in the ionosphere coincident with the ray paths to the interferometer. Thus, for each antenna, it is necessary to map a measurement

made along one ray path to the ray paths used by the interferometer. Many different techniques to do this mapping have been suggested and tried; all of them of dubious accuracy. In the light of these problems, and in the anticipation that dual-frequency observations will be employed for the most accurate interferometric work, we have implemented only a simple hour-angle mapping of the time history of the measurements of I_e at a given latitude and longitude to the point of interest. In this model we allow the user to adjust the "height", h, of the ionosphere, but require

$$h_1 = h - 35 \text{ km}$$
$$h_2 = h + 70 \text{ km} \tag{5.24}$$

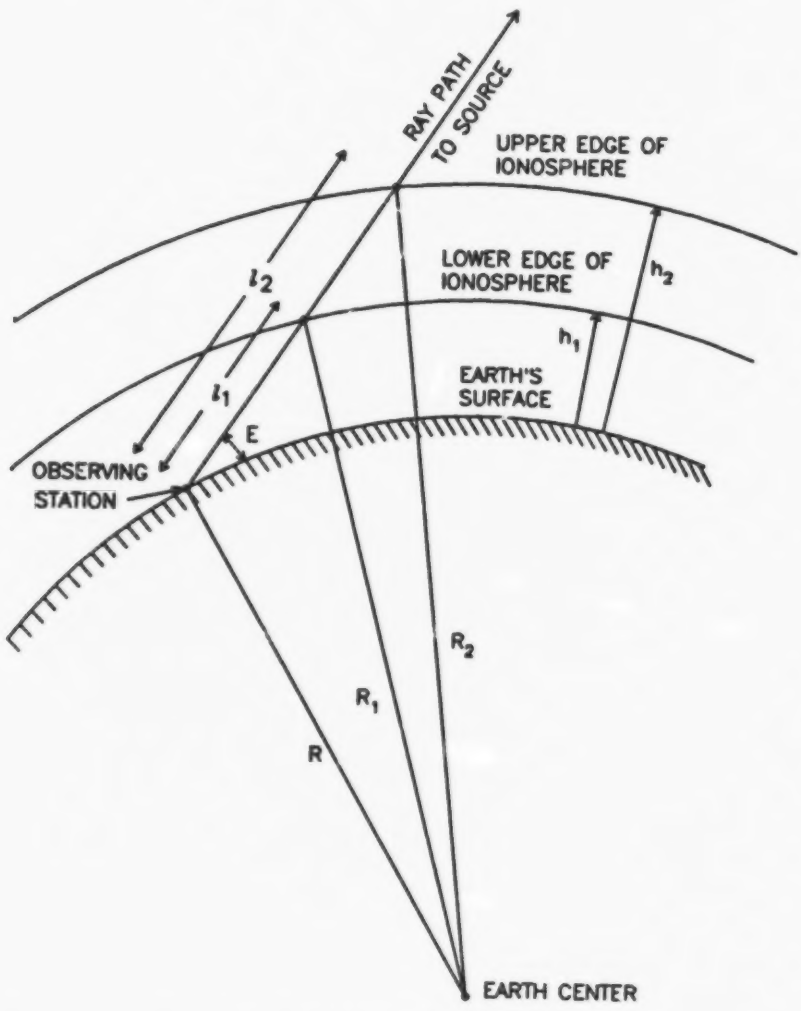

Figure 7. The geometry of the spherical ionospheric shell used for ionospheric corrections

Nominally, this "height" is taken to be 350 km. Setting this height to zero causes the program to ignore the ionosphere model, as is required if dual-frequency observations have already been used to remove the plasma effects. As in the troposphere model, these corrections can also be incorporated into, and passed in the input data stream. Then the user is free to accept the passed correction,

and use this model as a small alteration of the previously invoked model, or to remove the passed corrections.

The deficiencies of these ionosphere models for single-frequency observations are compounded by the lens effect of the solar plasma. In effect, the Solar System is a spherical plasma lens which will cause the apparent positions of the radio sources to be shifted from their actual positions by an amount which depends on the solar weather and on the Sun-Earth-source angle. Since both the solar weather and the Sun-Earth-source angle change throughout the year, very accurate observations over the time scale of a year will be virtually impossible.

Again, this portion of the model is linear in the parameter $I_{e\ add}$. Thus, the partial with respect to that parameter is

$$\frac{\partial \tau}{\partial I_{e\ add}} = \frac{k\ f(\text{station \#})\ g(\text{data type})\ S(E)}{\nu^2} \tag{5.25}$$

with $f(2) = 1$ and $f(1) = -1$.

SECTION 6

MODELING THE PHASE DELAY RATE (FRINGE FREQUENCY)

The interferometer is capable of producing several data types: group delay, phase delay, and the time rate of change of phase delay. Actually, the time rate of change of group delay is also available. However, it is not accurate enough to be of significance for geodetic uses. The models discussed above are directly applicable either to group delay or to phase delay. However, the model for the time rate of change of phase delay (fringe frequency) must be either constructed separately, or its equivalent information content obtained by forming the time difference of two phase delay values constructed from the delay-rate measurements as shown below. We chose the latter route since then only models of delay are needed. The two phase delay values, $\tau_{pd}(t \pm \Delta)$, used to represent the delay-rate measurement information content are obtained from the expression

$$\tau_{pd}(t \pm \Delta) = \tau_m(t \pm \Delta) + \tau_r(t) \pm \dot{\tau}_r \Delta \tag{6.1}$$

where $\tau_m(t)$ is the model used in the delay extraction processing step, $\tau_r(t)$ is the residual of the observations from that model, and $\dot{\tau}_r$ is the residual delay rate of the data relative to that model. This modeling for the delay extraction step is covered in Thomas (1981), and is done in analysis steps prior to and completely separate from the modeling described in this report. The output of those previous steps is such that the details of all processing prior to the modeling described here are transparent to this step. Only total interferometer delays and differenced total interferometer phase delays (divided by the time interval of the difference) are reported to this step. One of the requirements of these previous processing steps is that the model delay used be accurate enough to provide a residual phase that is a linear function of time over the observation interval required to obtain the delay information. A linear fit to this residual phase yields the value of $\dot{\tau}_r$, the residual delay rate. Using these two values of τ_{pd}, obtained by (6.1) above, the quantity, R, is constructed by the following algorithm:

$$R = \frac{[\tau_{pd}(t + \Delta) - \tau_{pd}(t - \Delta)]}{2\Delta} \tag{6.2}$$

This value and the group delay measurement, τ_{gd}, are the two data types that normally serve as the interferometer data input to be explained by the model described in this report. The software, however, also has the option to model phase delay, τ_{pd}, directly. In the limit $\Delta \rightarrow 0$, this expression for differenced phase delay approaches the instantaneous time rate of change of phase delay (fringe frequency) at time t. In practice, Δ must be large enough to avoid roundoff errors that arise from taking small differences of large numbers, but should also be small enough to allow R to be a reasonably close approximation to the instantaneous delay rate. A suitable compromise appears to be $\Delta \approx 2$ seconds. Fortunately, Δ has a wide range of allowed values, and the capability to model interferometer performance accurately is relatively insensitive to this choice.

SECTION 7

PHYSICAL CONSTANTS USED

In the software that has been implemented we have tried to use the constants recommended by the IAU project MERIT (Melbourne et al., 1983). Those that have not been defined in the text above, but which have an effect on the results that are obtained using the JPL software, are given below:

Symbol	Value	Quantity
c	299792.458	Velocity of light (km/sec)
r_0	2.817938×10^{-15}	Classical radius of the electron (meters)
R_E	6378.140	Equatorial radius of the Earth (km)
ω_E	$7.2921151467 \times 10^{-5}$	Rotation rate of the Earth (rad/sec)
f	298.257	Flattening factor of the geoid
h	0.609	Vertical Love number
l	0.0852	Horizontal Love number

SECTION 8

POSSIBLE IMPROVEMENTS TO THE CURRENT MODEL

This section lists areas in which the current model can be improved.

Variations in the rates of the station clocks in the potential well of the Sun:

We estimate that the delay error is less than 0.6 cm for measurements of intercontinental baselines. As the accuracy of observations improves over the next few years, this portion of the model will be improved.

Earth Orientation Models:

The models we are using for the orientation of the Earth in space are very nearly the best available today. However, there are short-period deficiencies that may be as large as 1 to 2 milliarcseconds, and longer-term deficiencies of the order of 1 milliarcsecond per year (5 cm at one Earth radius). VLBI measurements made during the past few years indicate the need for revisions of the annual nutation terms and the precession constant that are of this order [Eubanks et al. (1985), Herring et al. (1986)]. The 18.6-year term in the IAU nutation series may also be in error, and present data spans are just approaching durations long enough to separate it from precession. To provide an improved nutation model, we have implemented a MASTERFIT option to use the amplitudes of Herring et al. (discussed at the end of Section 2.7). This will constitute a temporarily better model of the annual and semiannual nutations until the IAU series is officially revised.

Tidal Effects:

The octupole component of solid Earth tides is neglected in the present model. Payne (1986) estimates that it may contribute as much as 0.5 cm to intercontinental baseline lengths.

Antenna Deformation:

Gravity loading and temperature variations may cause variations in the position of the reference point of a large antenna that are as large as 1 to 2 cm. Liewer (1986) presents evidence that these effects cause systematic errors and that their dependence on antenna orientation and ambient temperature may be modeled.

Antenna Alignment:

Hour angle misalignment of the order of 1 arc minute can cause 1 mm delay effects for DSN HA-Dec antennas with 7-m axis offsets.

Subreflector Focusing:

For DSN 64-m Cassegrain antennas, allowing the subreflector to slew in order to maintain focus changes the path delay by $\approx$ 4 cm over the $6° - 90°$ elevation range. Simulations (Jacobs, 1987) show that this effect is almost entirely absorbed by the clock epoch and local station vertical coordinate parameters. For baselines between two 64-m antennas, this causes a potential error of up to 8 cm in length.

Tropospheric Effects:

For DSN HA-Dec antennas, the altitude of the declination axis can vary by up to 7 meters. This altitude variation, when scaled by a mapping function, causes variations of several millimeters in the observed delay. This effect may be detectable in phase delay observations currently being analyzed.

SECTION 9

REFERENCES

Agnew, D. C. (private communication to O. J. Sovers in 1982), University of California at San Diego, La Jolla, California.

Allen, S. L., "Mobile Station Locations", IOM 335.1-71 (JPL internal document), Jet Propulsion Laboratory, Pasadena, California, Dec. 6, 1982.

Aoki, S., B. Guinot, G. H. Kaplan, H. Kinoshita, D. D. McCarthy, and P. K. Seidelmann, "The New Definition of Universal Time", *Astron. Astrophys.*, Vol. 105, pp. 359-361, 1982.

Bureau International de l'Heure, Annual Report for 1981, Paris, France, 1982 (typical for all years).

Cannon, W. H., "A Survey of the Theory of the Earth's Rotation", *JPL Publication 82-38*, Jet Propulsion Laboratory, Pasadena, California, Nov. 1, 1981.

Chao, C. C., "The Troposphere Calibration Model for Mariner Mars 1971", *Technical Report 32-1587*, Jet Propulsion Laboratory, Pasadena, California, pp. 61-76, March, 1974.

Davis, J. L., T. A. Herring, I. I. Shapiro, A. E. E. Rogers, and G. Elgered, "Geodesy by Radio Interferometry: Effects of Atmospheric Modeling Errors on Estimated Baseline Length", *Radio Science*, Vol. 20, pp. 1593-1607, 1985.

Eubanks, T. M., J. A. Steppe, and M. A. Spieth, "The Accuracy of Radio Interferometric Measurements of Earth Rotation" *TDA Progress Report 42-80*, Jet Propulsion Laboratory, Pasadena, California, pp. 229-235, Oct.-Dec. 1984.

Eubanks, T. M., J. A. Steppe, and O. J. Sovers, "An Analysis and Intercomparison of VLBI Nutation Estimates", *Proc. Int. Conf. on Earth Rotation and the Terrestrial Reference Frame*, Ohio State University, Columbus, Ohio, Vol. 1, pp. 326-340, 1985.

Goad, C. C., in IAU, IUGG Joint Working Group on the Rotation of the Earth, "Project MERIT Standards", *United States Naval Observatory Circular No.167*, pp.A7-1 to A7-25, U.S. Naval Observatory, Washington, D.C., Dec. 27, 1983.

Herring, T. A., C. R. Gwinn, and I. I. Shapiro, "Geodesy by Radio Interferometry: Studies of the Forced Nutations of the Earth. Part I: Data Analysis", *J. Geophys. Res.*, Vol. 91, pp. 4745-4754, 1986.

International Association of Geodesy, International Radio Interferometric Surveying (IRIS) Bulletin A, no. 23, Jan., 1986.

Jackson, J. D., *Classical Electrodynamics*, John Wiley & Sons, Inc., New York, New York, p. 517, 1975.

Jacobs, C. S. (private communication to O. J. Sovers in 1987), Jet Propulsion Laboratory, Pasadena, California.

Kaplan, G. H., "The IAU Resolutions of Astronomical Constants, Time Scales, and the Fundamental Reference Frame", *United States Naval Observatory Circular No. 163*, U.S. Naval Observatory, Washington, D.C., Dec. 10, 1981.

Lanyi, G. E., "Tropospheric Delay Effects in Radio Interferometry", *Telecommunications and Data Acquisition Prog. Rept. 42-78*, pp. 152-159, Jet Propulsion Laboratory, Pasadena, California, April-June, 1984.

Lieske, J. H., T. Lederle, W. Fricke, and B. Morando, "Expressions for the Precession Quantities Based upon the IAU (1976) System of Astronomical Constants", *Astron. Astrophys.*, Vol. 58, pp. 1-16, 1977.

Liewer, K. M., "Antenna Rotation Corrections to VLBI Data", IOM 335.4-499 (JPL internal document), Jet Propulsion Laboratory, Pasadena, California, March 29, 1985.

Liewer, K. M. (private communication to O. J. Sovers in 1986), Jet Propulsion Laboratory, Pasadena, California.

Melbourne, W. G., J. D. Mulholland, W. L. Sjogren, and F. M. Sturms, Jr., "Constants and Related Information for Astrodynamic Calculations", *Technical Report 32-1306*, Jet Propulsion Laboratory, Pasadena, California, July 15, 1968.

Melbourne, W., R. Anderle, M. Feissel, R. King, D. McCarthy, D. Smith, B. Tapley, R. Vicente, "Project MERIT Standards", *United States Naval Observatory Circular No. 167*, U.S. Naval Observatory, Washington, D.C., Dec. 27, 1983.

Melbourne, W., R. Anderle, M. Feissel, R. King, D. McCarthy, D. Smith, B. Tapley, R. Vicente, "Project MERIT Standards", *United States Naval Observatory Circular No. 167, Update #1*, U.S. Naval Observatory, Washington, D.C., Dec. 1985.

Melchior, P., *The Earth Tides*, p. 114, Pergamon Press, New York, New York, 1966.

Minster, J. B., and T. H. Jordan, "Present-Day Plate Motions", *J. Geophys. Res.*, Vol. 33, pp. 5331-5354, 1978.

Moyer, T. D., "Mathematical Formulation of the Double-Precision Orbit Determination Program (DPODP)", *Technical Report 32-1527*, Jet Propulsion Laboratory, Pasadena, California, pp. 12-17, May 15, 1971.

Pagiatakis, S. D., "Ocean Tide Loading, Body Tide and Polar Motion Effects on Very Long Baseline Interferometry", *Technical Report No. 92*, Dept. of Surveying Engineering, University of New Brunswick, Fredericton, N. B., Canada, Dec. 1982.

Pagiatakis, S. D., R. B. Langley, and P. Vanicek, "Ocean Tide Loading: A Global Model for the Analysis of VLBI Observations", presented at the 3rd International Symposium on the Use of Artificial Satellites for Geodesy an l Geodynamics, National Technical University, Athens, Greece, Sept. 1982.

Payne, D. G. (private communication to O. J. Sovers in 1986), Jet Propulsion Laboratory, Pasadena, California.

Rabbel, W., and H. Schuh, "The Influence of Atmospheric Loading on VLBI Experiments", *J. Geophysics*, Vol. 59, pp. 164-170, 1986.

Resch, G. M., and R. B. Miller, "Water Vapor Radiometry in Geodetic Applications", *Geodetic Aspects of Electromagnetic Wave Propagation through the Atmosphere*, Ed. F. K. Brunner, Springer Verlag, Berlin, Germany, 1983.

Scherneck, H. G., "Crustal Loading Affecting VLBI Sites", University of Uppsala, Institute of Geophysics, Dept. of Geodesy, *Report No. 20*, Uppsala, Sweden, 1983.

Seidelmann, P. K., "1980 IAU Theory of Nutation: The Final Report of the IAU Working Group on Nutation", *Celestial Mechanics*, Vol. 27, pp. 79-106, 1982.

Spitzer, L., Jr., *Physics of Fully Ionized Gases*, Interscience Publishers, New York, New York, 1967.

Thomas, J. B., "Reformulation of the Relativistic Conversion between Coordinate Time and Atomic Time", *Astron. J.*, Vol. 80, pp. 405-411, May, 1975.

Thomas, J. B. (private communication to J. L. Fanselow in 1976), Jet Propulsion Laboratory, Pasadena, California.

Thomas, J. B., "An Analysis of Radio Interferometry with the Block 0 System", *JPL Publication 81-49*, Jet Propulsion Laboratory, Pasadena, California, 1981.

Wade, C. M., "Precise Positions of Radio Sources", *Astrophys. J.*, Vol. 162, p. 381, 1970.

Williams, J. G., "Solid Earth Tides", IOM 391-109 (JPL internal document), Jet Propulsion Laboratory, Pasadena, California, July 14, 1970.

Yoder, C. F., J. G. Williams, and M. E. Parke, "Tidal Variations of Earth Rotation", *J. Geophys. Res.*, Vol. 86, B2, pp. 881-891, 1981.

Yoder, C. F. (private communication to J. L. Fanselow in 1982), Jet Propulsion Laboratory, Pasadena, California.

Yoder, C. F. (private communication to O. J. Sovers in 1983), Jet Propulsion Laboratory, Pasadena, California.

Yoder, C. F. (private communication to O. J. Sovers in 1984), Jet Propulsion Laboratory, Pasadena, California.

APPENDIX A

EQUIVALENCE OF TWO METHODS OF CORRECTING FOR GRAVITATIONAL BENDING

The formulation for differential gravitational retardation should, in the limit of large distances from the object producing the gravitational well, produce the same "bending" of the light ray as that produced by the more commonly available formula for the bending, i.e.:

$$\Theta = \frac{2(1+\gamma_{PPN})\mu}{c^2 R} \tag{A.1}$$

Indeed it does, as has been shown by Thomas in a private communication (1976).
Assume the geometry in figure 3 where $\hat{\mathbf{r}}_s$ is the direction from the center of the gravitational mass to the source, now assumed to be at infinity, and R is the distance of closest approach of the light ray to the center of this object. Starting with (2.20), and making use of the two approximations:

$$\mathbf{r}_1 + \mathbf{r}_1 \cdot \hat{\mathbf{r}}_s \approx r_1 - |r_1^2 - R^2|^{1/2} \approx \frac{R^2}{2r_1} \tag{A.2}$$

and

$$\hat{\mathbf{r}}_1 + \hat{\mathbf{r}}_s = \hat{\mathbf{R}} R/r_1 \tag{A.3}$$

which hold for a source infinitely far away, we obtain:

$$\Delta_p = -\frac{(1+\gamma_{PPN})\mu_p}{c^3} \ln\left[1 + \frac{\Delta\mathbf{r}\cdot\hat{\mathbf{R}}(R/r_1)}{|R^2/(2r_1)|}\right] \approx -\frac{(1+\gamma_{PPN})\mu_p}{c^3}\frac{2\Delta\mathbf{r}\cdot\hat{\mathbf{R}}}{R} \tag{A.4}$$

If instead of using the above formulation, we altered the apparent direction of the source by an angle

$$\Theta = \frac{2(1+\gamma_{PPN})\mu}{c^2 R} \tag{A.5}$$

and calculated the resultant change in delay due to this apparent change in source position, we should obtain the same change in delay as Δ_p calculated above.
From figure 3:

$$\hat{\mathbf{r}}_s' = \frac{\hat{\mathbf{r}}_s + \Theta\hat{\mathbf{R}}}{|\hat{\mathbf{r}}_s + \Theta\hat{\mathbf{R}}|} \approx (\hat{\mathbf{r}}_s + \Theta\hat{\mathbf{R}})(1 - \Theta^2/2) \tag{A.6}$$

where we have made use of the fact that $\hat{\mathbf{r}}_s \cdot \hat{\mathbf{R}} = 0$. Since $\Theta \leq 10^{-5}$, we have to an accuracy of 10^{-5} arc seconds that

$$\hat{\mathbf{r}}_s' = \hat{\mathbf{r}}_s + \Theta\hat{\mathbf{R}} \tag{A.7}$$

Thus,

$$\tau' = -\Delta\mathbf{r}\cdot\hat{\mathbf{r}}_s'/c = -\Delta\mathbf{r}\cdot\hat{\mathbf{r}}_s/c - \Delta\mathbf{r}\cdot\hat{\mathbf{R}}\Theta/c \tag{A.8}$$

Since

$$\tau = -\Delta\mathbf{r}\cdot\hat{\mathbf{r}}_s/c \tag{A.9}$$

the additional delay, Δ_p, due to the bending is:

$$\Delta_p = -\frac{2\Delta\mathbf{r}\cdot\hat{\mathbf{R}}(1+\gamma_{PPN})\mu_p}{c^3 R} \tag{A.10}$$

which is identical to the expression (A.4) above for the additional delay due to the differential retardation. Notice that we have glossed over the motion of station #2 in this treatment. However, a complete treatment should give essentially the same result to the accuracy of the terms neglected in this treatment.

APPENDIX B

MASTERFIT PARAMETERS

For the convenience of users of MASTERFIT, Table B.I identifies the names of adjustable parameters in the code with the notation of this document. Brief definitions and either references to equations (in parentheses) or sections (no parentheses) are also given.

Table B.I

Glossary of MASTERFIT Parameters

Parameter	MASTERFIT name	Definition	Reference
r_{sp}	RSPINAX aaaaaaaa	Cylindrical	(2.37)
λ	LONGTUD aaaaaaaa	station	(2.38)
z	POLPROJ aaaaaaaa	coordinates	(2.39)
$\dot{r}_{sp}$	DRSP/DT aaaaaaaa	Time rates of	(2.37)
$\dot{\lambda}$	DLON/DT aaaaaaaa	change of	(2.38)
$\dot{z}$	DPOL/DT aaaaaaaa	stn. coords.	(2.39)
h, l	*LOVE # aaaaaaaa	Love numbers	(2.44)
ψ	TIDEPHZ aaaaaaaa	Tide lag	(2.50)
γ_{PPN}	GEN REL GAMMA FACTOR	PPN gamma	(2.16)
α	RIGHT ASCEN.ssssssssssss	Source RA	(2.171)
δ	DECLINATION ssssssssssss	Source dec.	(2.171)
$\Theta_{1,2}$	† POLE MOTION	Pole position	(2.65), (2.66)
$UT1 - UTC$	UT1 MINUS UTC	UT1 - UTC	2.6
$\delta\Theta_{x,y,z}$	‡ AXIS TWEAK OFFSET	Perturbation	(2.112)
$\delta\dot{\Theta}_{x,y,z}$	‡ AXIS TWEAK RATE	coefficients	(2.112)
A_{0j}	NUTATION AMPLTD PSI cjjj	Nutation	(2.87) to
A_{1j}	NUTATION AMPLTD PSITcjjj	amplitudes	(2.92)
$A_{2j,3j}$	NUTATION AMPLTD PSIA		
B_{0j}	NUTATION AMPLTD EPS cjjj		
B_{1j}	NUTATION AMPLTD EPSTcjjj		
$B_{2j,3j}$	NUTATION AMPLTD EPSA		

* V or H
† X or Y
‡ X, Y or Z
aaaaaaaa station name
ssssssssssss source name
c component: S, C for sine, cosine
jjj Wahr series term number

Table B.I cont.

Glossary of MASTERFIT Parameters

Parameter	MASTERFIT name	Definition	Reference
τ_{c1}	C EPOCH aaaaaaaa	Coefficients	(3.1)
τ_{c2}	C RATE aaaaaaaa	in clock	(3.1)
τ_{c3}	DCRAT/DTaaaaaaaa	model for	(3.1)
τ_{c4}	F OFFSETaaaaaaaa	delay and	(3.2)
τ_{c5}	F DRIFT aaaaaaaa	delay rate	(3.2)
ρz_{dry}	DRYZTROPaaaaaaaa	Dry zenith delay	(4.3)
ρz_{wet}	WETZTROPaaaaaaaa	Wet zenith delay	(4.3)
$\dot{\rho} z_{dry}$	DDTRP/DTaaaaaaaa	Zenith delay	(4.4)
$\dot{\rho} z_{wet}$	DWTRP/DTaaaaaaaa	time rates	(4.4)
A_{dry}	DRYZMAPAaaaaaaaa	Chao map	(4.7) to
B_{dry}	DRYZMAPBaaaaaaaa	parameters	(4.11)
p	DRYMAPSGaaaaaaaa	Lanyi map parameter	(4.30)
T_0	SURFTEMPaaaaaaaa	CfA map surface temperature	(4.36)
$I_{e\ add}$	Z TECADDaaaaaaaa	Zenith electron content	(5.23)

aaaaaaaa station name